

# UC Santa Cruz

## UC Santa Cruz Previously Published Works

### Title

Nutrient strengthening and lead alleviation in Brassica Napus L. by foliar ZnO and TiO<sub>2</sub>-NPs modulating antioxidant system, improving photosynthetic efficiency and reducing lead uptake.

### Permalink

<https://escholarship.org/uc/item/092970jq>

### Journal

Scientific Reports, 14(1)

### Authors

Sehrish, Adiba  
Ahmad, Shoaib  
Alomrani, Sarah  
et al.

### Publication Date

2024-08-21

### DOI

10.1038/s41598-024-70204-0

### Copyright Information

This work is made available under the terms of a Creative Commons Attribution License, available at <https://creativecommons.org/licenses/by/4.0/>

Peer reviewed



OPEN

## Nutrient strengthening and lead alleviation in *Brassica Napus* L. by foliar ZnO and TiO<sub>2</sub>-NPs modulating antioxidant system, improving photosynthetic efficiency and reducing lead uptake

Adiba Khan Sehrish<sup>1</sup>, Shoaib Ahmad<sup>1</sup>, Sarah Owdah Alomrani<sup>2</sup>, Azeem Ahmad<sup>3</sup>, Khalid A. Al-Ghanim<sup>4</sup>, Muhammad Ali Alshehri<sup>5</sup>, Arslan Tauqeer<sup>6</sup>, Shafaqat Ali<sup>7,8</sup>✉ & Pallab K. Sarker<sup>9</sup>✉

With the anticipated foliar application of nanoparticles (NPs) as a potential strategy to improve crop production and ameliorate heavy metal toxicity, it is crucial to evaluate the role of NPs in improving the nutrient content of plants under Lead (Pb) stress for achieving higher agriculture productivity to ensure food security. Herein, *Brassica napus* L. grown under Pb contaminated soil (300 mg/kg) was sprayed with different rates (0, 25, 50, and 100 mg/L) of TiO<sub>2</sub> and ZnO-NPs. The plants were evaluated for growth attributes, photosynthetic pigments, leaf exchange attributes, oxidant and antioxidant enzyme activities. The results revealed that 100 mg/L NPs foliar application significantly augmented plant growth, photosynthetic pigments, and leaf gas exchange attributes. Furthermore, 100 mg/L TiO<sub>2</sub> and ZnO-NPs application showed a maximum increase in SPAD values (79.1%, 68.9%). NPs foliar application (100 mg/L TiO<sub>2</sub> and ZnO-NPs) also substantially reduced malondialdehyde (44.3%, 38.3%), hydrogen peroxide (59.9%, 53.1%), electrolyte leakage (74.8%, 68.3%), and increased peroxidase (93.8%, 89.1%), catalase (91.3%, 84.1%), superoxide dismutase (81.8%, 73.5%) and ascorbate peroxidase (78.5%, 73.7%) thereby reducing Pb accumulation. NPs foliar application (100 mg/L) significantly reduced root Pb (45.7%, 42.3%) and shoot Pb (84.1%, 76.7%) concentration in TiO<sub>2</sub> and ZnO-NPs respectively, as compared to control. Importantly, macro and micronutrient analysis showed that foliar application 100 mg/L TiO<sub>2</sub> and ZnO-NPs increased shoot zinc (58.4%, 78.7%) iron (79.3%, 89.9%), manganese (62.8%, 68.6%), magnesium (72.1%, 93.7%), calcium (58.2%, 69.9%) and potassium (81.5%, 68.6%) when compared to control without NPs. The same trend was observed for root nutrient concentration. In conclusion, we found that the TiO<sub>2</sub> and ZnO-NPs have the greatest efficiency at 100 mg/L concentration to alleviate Pb induced toxicity on growth, photosynthesis, and nutrient content of *Brassica napus* L. NPs foliar application is a promising strategy to ensure sustainable agriculture and food safety under metal contamination.

<sup>1</sup>State Key Laboratory of Pollution Control and Resource Reuse, School of the Environment, Nanjing University, Nanjing 210023, Jiangsu, China. <sup>2</sup>Department of Biology, College of Science and Arts, Najran University, 66252 Najran, Saudi Arabia. <sup>3</sup>Soil and Water Chemistry Laboratory, Institute of Soil and Environment Sciences, University of Agriculture, Faisalabad, Pakistan. <sup>4</sup>Department of Zoology, College of Science, King Saud University, 11451 Riyadh, Saudi Arabia. <sup>5</sup>Department of Biology, Faculty of Science, University of Tabuk, 71491 Tabuk, Saudi Arabia. <sup>6</sup>School of Modern Engineering and Applied Sciences, Nanjing University, Nanjing Jiangsu 210023, China. <sup>7</sup>Department of Environmental Science, Government College University, Faisalabad, Faisalabad 38000, Pakistan. <sup>8</sup>Department of Biological Sciences and Technology, China Medical University, Taichung 40402, Taiwan. <sup>9</sup>Environmental Studies Department, University of California Santa Cruz, Santa Cruz, CA 95060, USA. ✉email: shafaqataligill@yahoo.com; psarker@ucsc.edu

**Keywords** Antioxidant activities, Chlorophyll contents, Gas exchange attributes, Nanoparticles, Nutrient contents, Reactive oxygen species (ROS)

Heavy metals (HMs) have emerged as a prominent class of environmental toxins among abiotic stresses<sup>1,2</sup>. The presence of HMs in soil seriously exacerbated food security due to their adverse effects on crop nutritional quality. Global crop output is insufficient to meet the nutritional needs of the growing global population and due to increasing food demands, it is inevitable to grow crops in mild contaminated soils<sup>3</sup>. The accumulation of HMs in plant tissues through the food chain can pose a significant risk to both human and animal populations. When the concentration of HMs exceeds specific threshold levels, molecular, physiological, and biochemical processes within the plant alter as a response to stress<sup>4–6</sup>.

Lead (Pb) is classified as carcinogenic and the second most harmful heavy metal due to its non-degradability in nature<sup>7,8</sup>. Pb contamination in soil from natural and anthropogenic sources harms soil biota, environment, and humans without any beneficial impact on any of them<sup>9</sup>. Both stable and isotopic forms of lead (Pb) can accumulate in different plant parts and negatively affect crop quality<sup>10</sup>. The invasion of Pb with plants disrupts physiological functions and causes deleterious impacts on plants by disrupting basic plant metabolic processes and ultimately leading to the generation of reactive oxygen species (ROS) such as hydrogen peroxide (H<sub>2</sub>O<sub>2</sub>) and superoxide (O<sub>2</sub><sup>-</sup>), that are very crucial to plant physiology and morphology<sup>8,11,12</sup>. Higher levels of Pb cause structural changes in the photosynthetic apparatus and reduce the biosynthesis of chlorophyll pigments, leading to impaired carbon metabolism<sup>13</sup>. In addition, Pb can enter the human body through the food chain and interfere with the neurological system, gastrointestinal system, renal organs, and reproductive system<sup>14</sup>. Alleviating lead toxicity with increasing crop quality is of great importance to ensure food safety and agriculture production.

Nanotechnology has the potential to benefit the agri-food sector by reducing the toxicity of biotic and abiotic stresses and providing innovative solutions for sustainable agricultural production<sup>15,16</sup>. Many studies reported that nanoparticles (NPs) at the optimum concentration enhance crop production mitigating heavy metal induced toxicity by limiting their uptake and reducing accumulation<sup>17,18</sup>. However, some studies reported adverse effects of NPs at high concentrations<sup>19</sup>. Titanium oxide nanoparticles (TiO<sub>2</sub>-NPs) and zinc oxide NPs (ZnO-NPs) are widely used in both agriculture and industrial sectors among other metallic NPs<sup>20</sup>. Titanium (Ti) is a beneficial element for crops and titanium-based NPs reportedly improve crop productivity, photosynthetic efficiency, nutrient accessibility<sup>21</sup> antioxidant defense systems<sup>22</sup>, and alter gene expression of plants<sup>23</sup>. Further, TiO<sub>2</sub>-NPs greatly increased the growth, photosynthetic activity, and Cd tolerance in *Brassica juncea* L. plants under 10 mg/kg cadmium contaminated soil<sup>24</sup> and improved the plant development, photosynthetic efficiency, and antioxidant defense mechanism by inhibiting chromium absorption in *Helianthus annuus* L. reducing Pb bioaccumulation<sup>25</sup>, and enhanced macronutrient concentration<sup>26</sup>. Zinc (Zn) is a micronutrient and its application promptly cause various, physiological, biochemical, and molecular changes<sup>20</sup>, and improves plant growth and quality by reducing the bioavailability of heavy metals in plants<sup>27</sup>. ZnO-NPs foliar application remarkably improved the rice plants antioxidant enzyme activities i.e., catalase (CAT), Ascorbate peroxidase (APX), peroxidase (POD), and modulated nutrient homeostasis under arsenic stress<sup>28</sup>. Another study found that ZnO-NPs supplementation substantially improved growth, biomass, and mineral nutrients and efficiently reduced oxidative damage induced by Cd stress<sup>29</sup>.

*Brassica napus* L. is an important oilseed crop in Pakistan because of its contribution to current edible oil production and it is an important source of nutrients for humans and animals. Heavy metals might impact nutrient absorption in *Brassica juncea* L. and *Brassica napus* L. by competing for common enzyme binding sites, as documented by Feigl et al.<sup>30</sup>. Whilst it is well known that TiO<sub>2</sub> and ZnO-NPs improve plant growth, but role of these NPs, particularly in *Brassica napus* L. under Pb stress has not been well investigated. Keeping in view the importance of this crop and the usefulness of these NPs in the mitigation of HMs, the current study aimed to evaluate the efficacy of TiO<sub>2</sub> and ZnO-NPs role in alleviating Pb toxicity in *Brassica napus* L. plants by estimating Pb accumulation, and morphological physiological parameters under Pb contaminated soil. In addition, antioxidant enzyme activities and oxidants were also analyzed. The ultimate goal of this study is to explore TiO<sub>2</sub> and ZnO-NPs efficacy in strengthening nutrient content with alleviation of Pb toxicity in *Brassica napus* L. which is an important socioeconomic crop. The present findings provide insight into the practical applications of TiO<sub>2</sub> and ZnO-NPs in improving crop yield and nutrient strengthening under heavy metal stress, especially Pb.

## Material and methods

### ZnO and TiO<sub>2</sub> nanoparticles preparation and characterization

TiO<sub>2</sub>-NPs were prepared by a sol-gel method with slight modification<sup>31</sup>. In brief, titanium tetra chloride (TiCl<sub>4</sub>) was added to deionized water with stirring at 1000 rpm. Ammonia (NH<sub>3</sub>) solution was added gradually (dropwise) to adjust the pH (7.8) of the solution with continuous stirring until the gel was formed. Once the TiOH<sub>2</sub> colloidal sediments were formed, the sediments were then separated by filtration and dried at 70 °C (24 h). It was then heated to 400 °C and calcination was carried out (4 h) in the Environmental Toxicology & Chemistry lab at Government College University (GCU), Faisalabad, Punjab, Pakistan.

Zinc acetate dihydrate (Zn (CH<sub>3</sub>COO)<sub>2</sub>·2H<sub>2</sub>O) ≥ 99%, methanol (CH<sub>3</sub>OH), and Sodium Hydroxide (NaOH) 117 ≥ 99% and Nitride Chloride TiCl<sub>4</sub> (≥ 99.0%), Ammonia (NH<sub>3</sub>) was purchased from Alfa Aesar, Karlsruhe, Germany. The synthesis of zinc nanoparticles (ZnO-NPs) was carried out using a sol-gel method with minor modifications, as described by Vishwakarma and Sing<sup>32</sup>. To prepare a sol, zinc acetate dihydrate was dissolved with methanol at room temperature. Subsequently, the solution was subjected to ultrasonication at 25 °C for 120 min. A clear transparent sol was obtained with no precipitate and turbidity. Sodium Hydroxide (NaOH) 0.02 M solution, was added dropwise and ultrasonically stirred for 60 min. Following this, filter and wash the

precipitate with excess methanol to eliminate impurities. Precipitates were dried on a hot plate at 80 °C temperature for 15 min. The precipitates were annealed at 400 °C for 30 min.

#### Instrumental analysis

Scanning electron microscope (SEM) (German ZEISS Sigma 300) was performed to analyze nanoparticles surface morphology. The X-ray diffraction (XRD) data for ZnO-NPs and TiO<sub>2</sub>-NPs was obtained using a Bruker D8 Advance X-ray diffractometer, which was equipped with radiation and operated in the 2-theta range of 25–65°. FTIR-Thermo Scientific Nicolet iS20) was done to identify various functional groups in nanoparticles.

#### Soil sample collection and analysis

The soil used in this experiment was collected from the agriculture field of the University of Agriculture, Faisalabad, Punjab, Pakistan (31°26'18.1"N 73°04'10.5" E). Soil samples were collected from the surface (0–200 mm) using a scoop shovel, dried in the air, and sifted through a 2 mm sift for analysis and pot culturing. Physicochemical properties of soil were determined such as soil texture (silt clay), pH (7.80), Zn (0.453 mg kg<sup>-1</sup>), electrical conductivity (6.71 dS m<sup>-1</sup>), SAR (22 mmol L<sup>-1</sup>), Ca<sup>2+</sup> + Mg<sup>2+</sup> (18 meq L<sup>-1</sup>), available phosphorous (2.78 mg kg<sup>-1</sup>), and available Pb (21.23 mg kg<sup>-1</sup>).

#### Plant materials and growth conditions

A pot experiment was conducted in a natural environment (day/night 23.3/16 °C, relative humidity 39 ± 3%) in a botanical garden at GC University, Faisalabad, Punjab, Pakistan. The pots used for the experiment were cylindrical plastic pots (130 g, 7.8 cm diameter, 8.7 cm height). The experiment was carried out under a completely randomized design (CRD) with three replicates. The soil was spiked with Pb using Lead acetate Pb(C<sub>2</sub>H<sub>3</sub>O<sub>2</sub>)<sub>2</sub> at a loading rate of 300 mg/kg and incubated for two months for Pb stabilization. Each pot was filled with five kg of spiked soil. Seeds of *Brassica napus* L. (cv. Super Canola) were purchased from Ayub Agricultural Research Institute, Faisalabad (AARI) and disinfected with hydrogen peroxide (2.5% v/v) solution for 20 min and again washed with distilled water (DW). Seeds were incubated in darkness at 25 °C for three days before sowing in the pot. Seven seeds/pots were sown and after germination thinning was done retaining 3 plants/pots. The recommended dose of NPK (120:80:40 kg/ha) was applied to avoid nutrient deficiency. NPs were applied after one week of germination and before foliar application, NPs were ultra-sonicated for 30 min with distilled water to disperse properly at 0, 25, 50, and 100 mg/L concentrations according to the treatment plan. In total, six sprays were applied to each treatment, and at the same time, control plants were sprayed with DW. During the growing period, the plants were irrigated using tap water with a pH value of 7.42, as measured by a pH meter (Portable Meter Hanna HI-9812-51).

#### Measurement of growth parameters

After harvesting, growth parameters including height (cm) of the plant (shoot length, root length) and fresh and dry weight were determined after separating the plant into different parts. Plant dry weight was measured after drying the plant parts oven (72 h at 70 °C) and ground into fine powder for further analysis. The length of plant parts was measured with a stainless meter rod and weight with an electric weight balance.

#### Measurement of Photosynthetic pigment and SPAD values

To determine the concentration of chlorophyll, plant leaves weighing 0.15 g, were crushed. The resulting crushed leaves were then placed into a testing tube (10 mL) containing 4 mL of a buffer solution (1:1 ratio) containing ethanol and acetone. Subsequently, the tube was incubated in darkness for 5 h. The centrifugation was performed at 3000 rpm for 10 min to collect the supernatant and measured by spectrophotometer (Labman LMSPUV1900 Double Beam UV-VIS Spectrophotometer)<sup>33</sup>. Equations used to calculate chlorophyll and carotenoid content:

$$\text{Chlorophyll a } (\mu\text{g/ mL}) = 10.3 * E_{663} - 0.98 * E_{644}$$

$$\text{Chlorophyll b } (\mu\text{g/ mL}) = 19.7 * E_{644} - 3 : 87 * E_{663}$$

$$\text{Total chlorophyll } (\mu\text{g/ mL}) = \text{chlorophyll a} + \text{chlorophyll b}$$

$$\text{Total carotenoids } (\mu\text{g/ mL}) = 4.2 * E_{452} - \{ (0.0264 * \text{Chl a}) + (0.426 * \text{Chl b}) \}$$

The SPAD value of leaves was determined with a portable SPAD meter (atLEAF CHL STD chlorophyll meter 502). In addition, an Infrared gas analyzer (3051c Plant photosynthesis meter Hangzhou Chincan Trading Co., Ltd) was used to record the leaf gas exchange parameters on a sunny (10: am to 11: am). The calibration of the Portable Infra-Red Gas Analyzer was conducted at different scales, including air temperature (20 °C), relative humidity (60%), and ambient CO<sub>2</sub> concentration (400 ppm). Fully extended second flag leaves were chosen from each pot to measure the stomatal conductance (G<sub>s</sub>), transpiration rate (Tr), photosynthetic rate (Pn), and water use efficacy (WUE) was measured. Water use efficiency was calculated as  $WUE = Pn/Tr$ .

#### Determination of antioxidant enzymes and oxidants

To prepare antioxidant enzyme extract, leaf samples were ground using a pre-cooled pestle and mortar in a phosphate buffer solution (PBS) with a pH of 7.8. The homogenized mixture was centrifuged to obtain a supernatant (enzyme extract) for antioxidant enzyme activity analysis. Peroxidase (POD) activity and superoxidase (SOD) activity was measured according to Zhang<sup>34</sup>. For POD activity, enzyme extract was added to PBS and 300 mM of hydrogen peroxide (H<sub>2</sub>O<sub>2</sub>) and measured with a spectrophotometer. To determine SOD activity the reaction

solution was prepared with enzyme extract, L-methionine, riboflavin, and NBT, with EDTA- $\text{Na}_2$  and quantified using a spectrophotometer. Catalase (CAT) activity was measured by Aebi<sup>35</sup>. The APX was determined by following the method of Nakano and Asda<sup>36</sup>. The analysis of malondialdehyde (MDA) in plant tissues was determined according to the method described by Heath and Packer<sup>37</sup>. In brief, the leaf sample (0.5 g) was homogenized with 0.5% thiobarbituric acid (TBA) and added with 20% TCA solution. To determine  $\text{H}_2\text{O}_2$  content, the leaf sample was pulverized in a TCA solution by adopting the method proposed by Jana and Choudhuri<sup>38</sup>. The electrolyte leakage (EL) in the leaves was determined according to the modified method described by Dionisio-Sese and Tobita<sup>39</sup>. The EL was calculated by the ratio of the percentage of  $\text{EC}_1$  to  $\text{EC}_2$  as follows:

$$\text{Electrolyte Leakage \%} = (\text{EC}_1 / \text{EC}_2) * 100 \quad (1)$$

### Metal and nutrient estimation

To measure Pb concentration, and nutrient content the plant roots and shoot samples (0.5 g) were acid digested with  $\text{HNO}_3$ :  $\text{HClO}_4$  (3:1 v/v) solution on a hot plate and after digestion filtered through 0.22  $\mu\text{m}$  filters<sup>40</sup>. The filtered samples were subsequently used to measure Pb and nutrient concentrations in the samples using ICP-OES (Optima 7000DV ICP-OES, Perkin Elmer).

### Statistical analyses

The data was analyzed using IBM SPSS Statistics (V20) with one-way analysis of variance (ANOVA) on mean values from three replicates and graphs were plotted by MS Excel (version, 2019). Tukey (HSD) test at 95% probability was employed to analyze the significance of the treatments. The alphabets were used to denote significant and non-significance variations among treatments.

## Results

### ZnO and $\text{TiO}_2$ nanoparticles characterization

SEM analyses showed the size, shape, and structure of the synthesized nanoparticles (NPs). SEM image of ZnO-NPs showed the hexagonal shape, uniform distribution, and nanoscale range at 10.00 k $\times$  and 500.00 k $\times$  magnification as demonstrated by their micrographs, and with particle size 65.29 nm (Fig. 1a–c). The EDX spectra of the NPs demonstrated the presence of Zn and O confirming the purity of obtained NPs as shown in Fig. 1d. ZnO-NPs showed phases in all XRD patterns. All of peaks observed at 2 theta positions were 31.732°, 34.364°, 36.207°, 47.469°, 56.526°, 62.754°, 67.851°, 68.995° along with their corresponding reflected planes (100), (002), (101), (102), (110), (103), (112), (201) respectively with JCPDS No. 01–080–0074. The XRD pattern of prepared ZnO-NPs is shown in Fig. 1e. The FTIR spectra of ZnO-NPs findings are shown in Fig. 1f. The observed peaks indicate the functional group that is typical for the ZnO-NPs. The absorption peaks were determined to lie between 3438.47  $\text{cm}^{-1}$ , 1633.01  $\text{cm}^{-1}$ , 1383.67  $\text{cm}^{-1}$ , 1120.55  $\text{cm}^{-1}$ . The absorption peak at 496.06  $\text{cm}^{-1}$  is due to the presence of metal oxide nature in the Zn–O vibration mode<sup>41</sup>.

Under SEM,  $\text{TiO}_2$ -NPs have predominantly spherical-shaped clusters with adequate dispersion, and clean shape and were evenly distributed at 5.00 k $\times$  and 50.00 k $\times$  magnification with particle size 41.21 nm (Fig. 2a–c). Compositional analysis  $\text{TiO}_2$ -NPs of by EDX demonstrated the presence of Ti and O (Fig. 2d). The XRD pattern of  $\text{TiO}_2$ -NPs peaks observed at 2 theta positions were 25.335°, 38.611°, 48.104°, 53.921°, 55.138 along with their corresponding reflected planes (101), (112), (200), (105), (211) respectively with JCPDS No. 01–083–2243. The crystal system of the prepared  $\text{TiO}_2$  nanostructure is tetragonal given in (Fig. 2e). The FTIR spectrum of titanium oxide nanoparticles are shown (Fig. 2f). The absorption peaks indicate the functional group was determined to lie between the range of 400.63–4000  $\text{cm}^{-1}$ . The broad peak at 3413.59  $\text{cm}^{-1}$  was related to the interaction of the hydroxyl group (–OH) attached to Ti. The 1632.24 peak corresponds to the –OH bending vibration. The broad peak at 400.63  $\text{cm}^{-1}$  is assigned to the bending vibration bonds (Ti–O–Ti)<sup>42</sup>.

### Effect of ZnO and $\text{TiO}_2$ nanoparticles on growth parameters

Our results showed that the lowest growth in plants was observed in treatment without any supplementation of NPs (NPs-0) indicating the negative effect of Pb on plant growth. However,  $\text{TiO}_2$ -NPs and ZnO-NPs foliar application in dose additive manner enhanced growth rate of *Brassica napus* L. grown under Pb contaminated soil as shown in (Fig. 3). Specifically, shoot and root length grown in Pb contaminated soil significantly ( $p \leq 0.05$ ) enhanced in NPs 100 mg/L treatment by 82.3% and 74.1% in  $\text{TiO}_2$  and 75.1% and 63.4% in ZnO-NPs respectively, as compared to control (NPs-0). Similarly, when compared with the control without NPs, the application of  $\text{TiO}_2$ -NPs and ZnO-NPs led to significant enhancement in root fresh weight and root dry weight which was 77.7%, 85.3% for 100 mg/L  $\text{TiO}_2$ -NPs and 61.4%, 76.6% for 100 mg/L ZnO-NPs treatment respectively, as compared to control (NPs-0). The shoot fresh weight and shoot dry weight dramatically increased up to 68.9% and 89.1% by foliar spray of 100 mg/L  $\text{TiO}_2$ -NPs up to 57.8% and 78.7% by application of ZnO-NPs respectively, as compared to control treatment (NPs-0). The maximum number of leaves was also observed in 100 mg/L  $\text{TiO}_2$ -NPs 93.3% and 100 mg/L ZnO-NPs 91.5% as compared to control (NPs-0) (Fig. 4). Overall, our results showed that NPs reversed the adverse effects of Pb toxicity and dramatically increased all growth indices compared to plants grown under only Pb stress without NPs treatment.

### Effect of $\text{TiO}_2$ and ZnO nanoparticles on photosynthetic pigment

$\text{TiO}_2$  and ZnO-NPs foliar application showed a positive influence on the photosynthetic pigments of plants under Pb stress. The maximum ( $p \leq 0.05$ ) increase in photosynthetic activity was observed in 100 mg/L NPs treatment (Fig. 5). An increase in Chlorophyll a was found at  $\text{TiO}_2$  and ZnO-NPs 100 mg/L by 66.5% and 62.8% respectively,

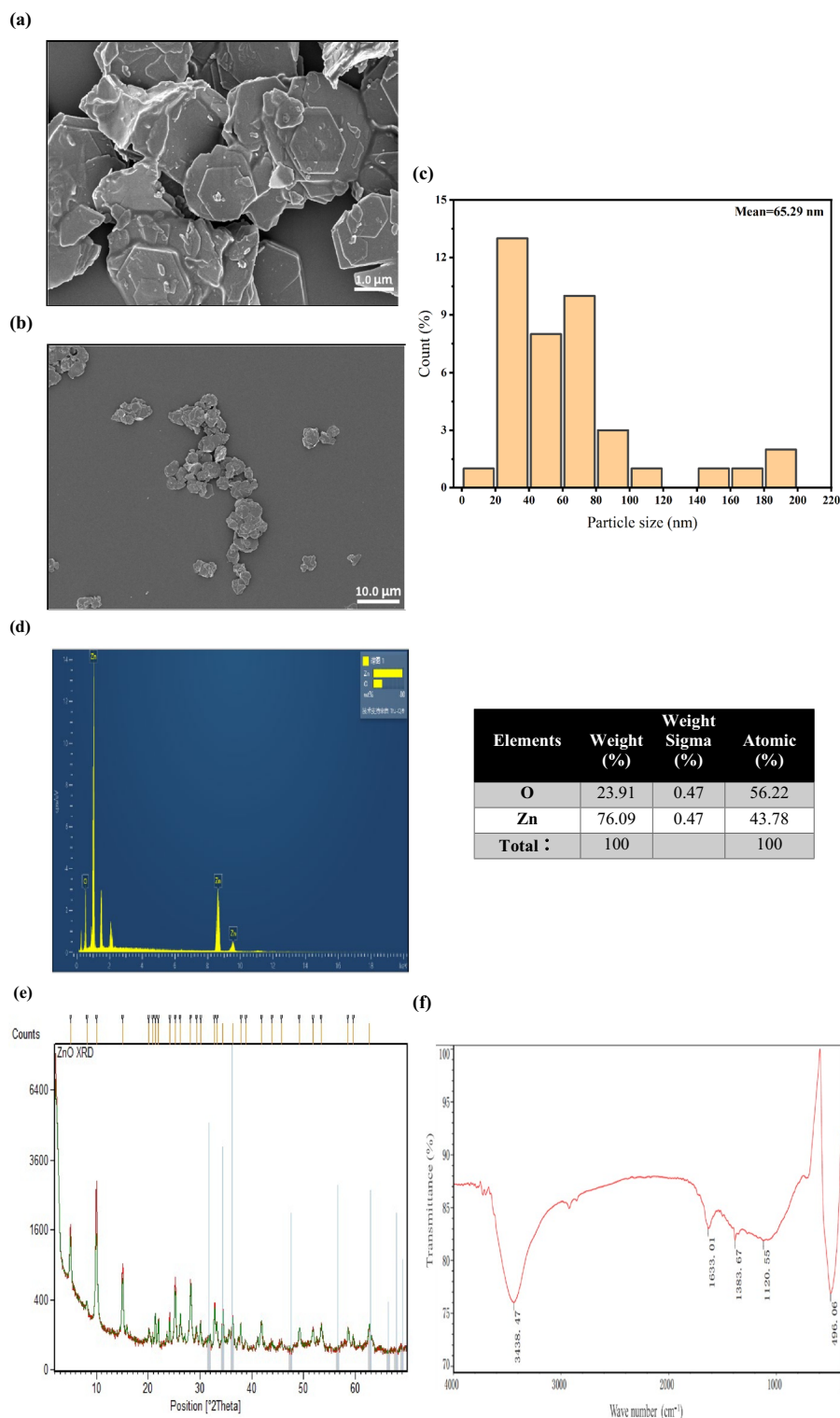


**Figure 1.** SEM images (a, b), Particle size distribution (c), EDX (d), XRD (e), and FTIR (f) of ZnO-NPs.

as compared to control (NPs-0). Likewise, chlorophyll b was increased by 86.3% and 77.3% at higher TiO<sub>2</sub>-NPs and ZnO-NPs (100 mg/L) respectively, as compared to the control. A prominent increase in carotenoid content was also observed at 100 mg/L TiO<sub>2</sub>-NPs followed by 100 mg/L ZnO-NPs with increasing values of 89.7% and 76.8% respectively, as compared to control (NPs-0). The imperative role of TiO<sub>2</sub> and ZnO-NPs was also observed in improving SPAD values. The highest SPAD value was found as 52.09 at 100 mg/L TiO<sub>2</sub> followed by 100 mg/L ZnO-NPs 49.14 and 50 mg/L TiO<sub>2</sub>-NPs (45.4) and 50 mg/L ZnO-NPs (43.9), which was 79.1%, 68.7%, 56.8%, 44.9% higher than control (NPs-0), respectively (Fig. 5).

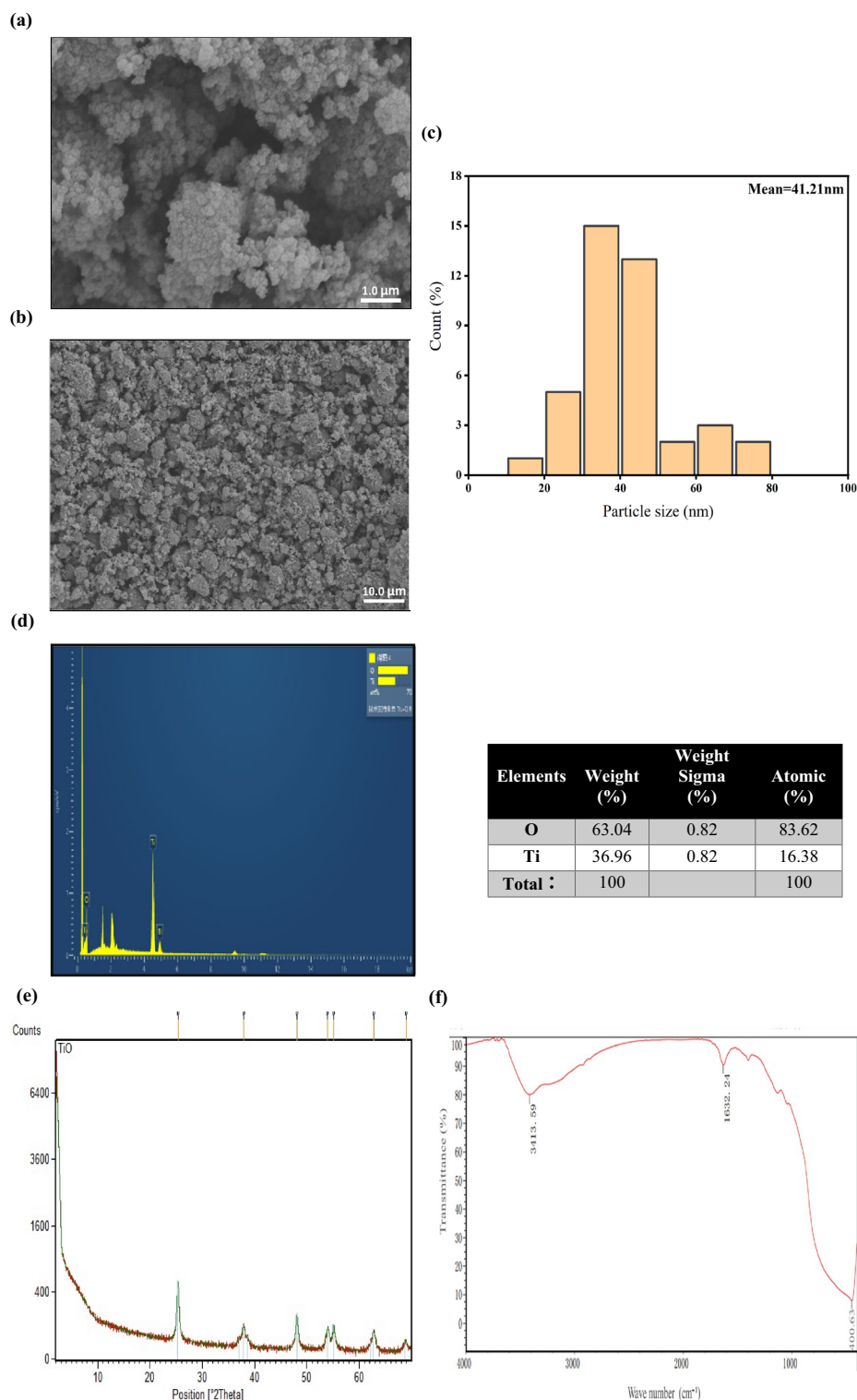


**Figure 2.** SEM images (a, b), Particle size distribution (c), EDX (d), XRD (e), and FTIR (f) of TiO<sub>2</sub>-NPs.

### Effect of TiO<sub>2</sub> and ZnO nanoparticles gas exchange parameters

The results depicted that plants treated with TiO<sub>2</sub>-NPs and ZnO-NPs substantially increased gas exchange parameters. When compared with control (NPs-0) all treatments with NPs boosted gas exchange metrics (Table 1). At 50 mg/L TiO<sub>2</sub> and ZnO-NPs concentration, the percent increase of the photosynthetic rate (*Pn*), transpiration rate (*Tr*), water use efficiency (*WUE*) and stomatal conductance (*Gs*) in plant under Pb stress was 70.8%, 75.4%, 71.5%, 69.3% and 50.7%, 63.1, 66.8%, 65.6%, 59.4% respectively, as compared to control (NPs-0). However, the maximum increase in photosynthetic rate (86.7%, 77.67%), transpiration rate (89.3%, 79.5%), water use

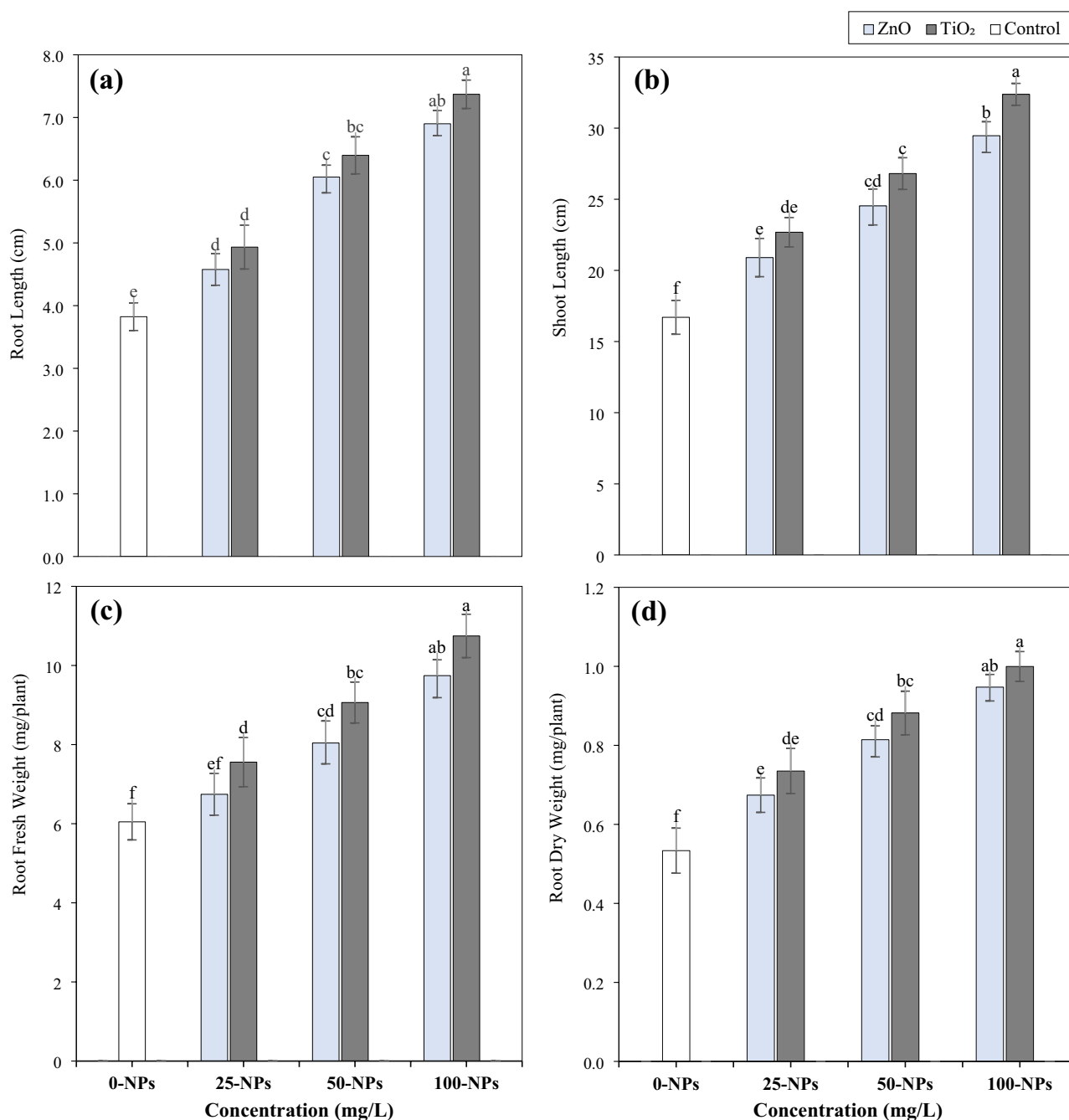


**Figure 3.** Effect of ZnO-NPs and TiO<sub>2</sub>-NPs on root length (a), shoot length (b), root fresh weight (c), and root dry weight (d) of *Brassica napus* L. grown under lead contaminated soil. The vertical bar on the graph demonstrates the standard deviation. Data are presented as values of three independent replicates, where each replicate constituted three plants per pot  $\pm$  SD. Different letters on the bars indicate significant differences among treatments at  $p \leq 0.05$ .

efficiency (84.9%, 72.5%), and stomatal conductance (74.5%, 69.5%) in plants was observed at 100 mg/L TiO<sub>2</sub> and ZnO-NPs respectively, as compared to control without NPs (NPs-O). All measured gas exchange parameters showed a statically significant increase at 50 and 25 mg/L concentrations of NPs treatment but lower than other (100 mg/L) treatments.

#### Effect of TiO<sub>2</sub> and ZnO nanoparticles on oxidants and antioxidant enzymes activity

The results indicated that plants grown under Pb contaminated soil without any NPs treatment depicted oxidative stress as evident by the highest MDA, H<sub>2</sub>O<sub>2</sub>, and EL levels compared to NPs treated plants. The TiO<sub>2</sub> and ZnO-NPs significantly increased antioxidant enzyme activities of superoxidase (SOD), peroxidase (POD), catalase (CAT), and ascorbate peroxidase (APX) in leaves as shown in (Fig. 6). while, simultaneously reducing



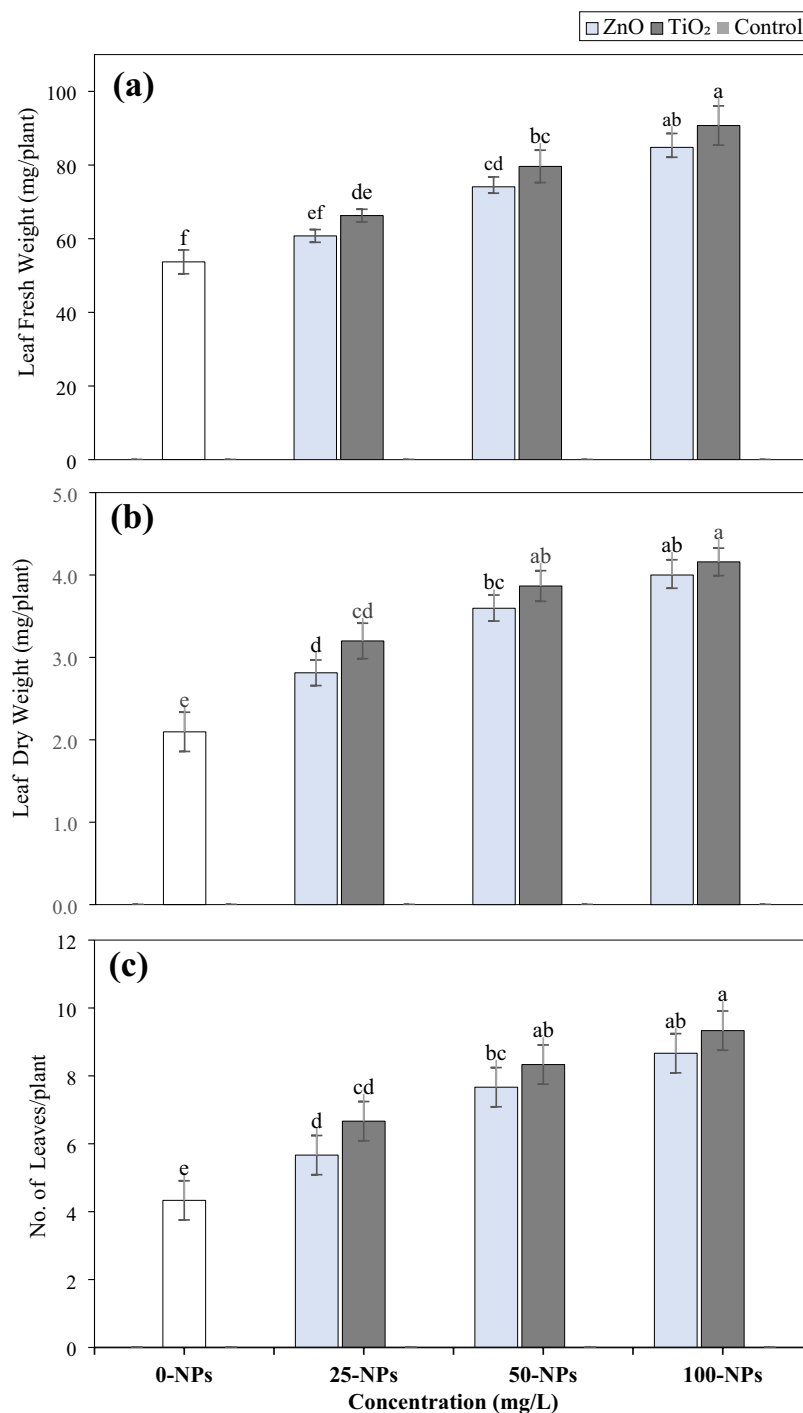


**Figure 4.** Effect of ZnO-NPs and TiO<sub>2</sub>-NPs on leaf fresh weight (a), leaf dry weight (b), and the number of leaves (c) of *Brassica napus* L. grown under lead contaminated soil. The vertical bar on the graph demonstrates the standard deviation. Data are presented as values of three independent replicates, where each replicate constituted three plants per pot  $\pm$  SD. Different letters on the bars indicate significant differences among treatments at  $p \leq 0.05$ .

the malondialdehyde (MDA), hydrogen peroxide (H<sub>2</sub>O<sub>2</sub>), and electrolyte leakage (EL) with increasing concentrations of NPs as depicted in (Fig. 7). The application of TiO<sub>2</sub> and ZnO-NPs at 100 mg/L significantly increased CAT (87.7%, 74.9%), SOD (83.8%, 79.8%), POD (87.8%, 76.9%) and APX (79.1%, 76.8%) activities respectively, as compared to control (NPs-0). Likewise, the maximum decrease in MDA (52.7%, 46.8%), H<sub>2</sub>O<sub>2</sub> (59.1%, 53.9%), and EL (74.2%, 68.7%) was observed at 100 mg/L TiO<sub>2</sub> and ZnO-NPs respectively, compared with control (NPs-0).

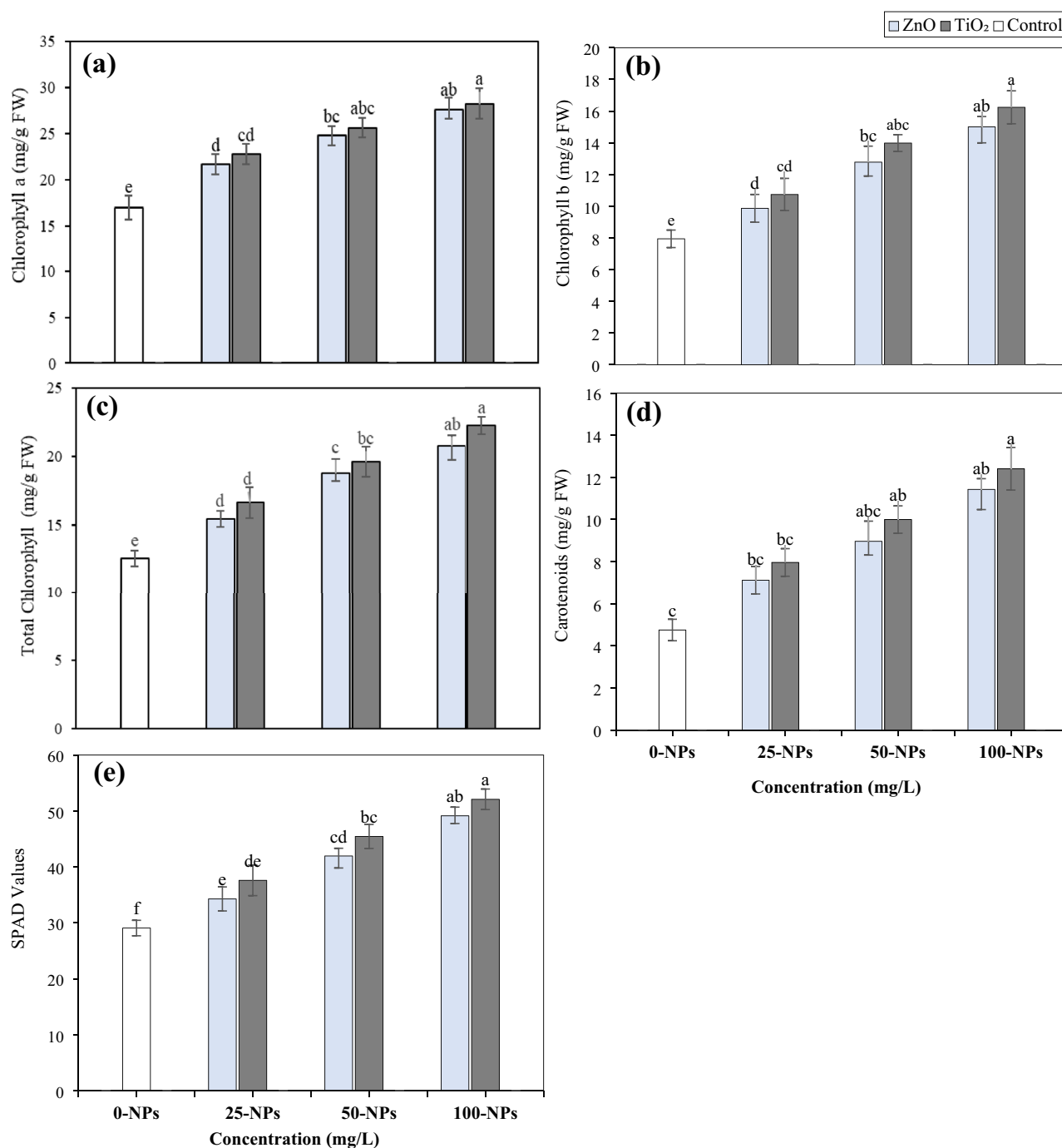


**Figure 5.** Effect of ZnO-NPs and TiO<sub>2</sub>-NPs on chlorophyll a (a), chlorophyll b (b), total chlorophyll (c), carotenoids (d) and SPAD values (e) of *Brassica napus* L. grown under lead contaminated soil. The vertical bar on the graph demonstrates the standard deviation. Data are presented as mean  $\pm$  SD (n = 3). Different letters on the bars indicate significant differences among treatments at  $p \leq 0.05$ .

### Pb accumulation and fractions in plant parts

The results depicted that Pb accumulation in plant parts diminished with increasing concentration of NPs (Fig. 8). The highest shoot and root Pb concentrations were estimated to be higher at control (NPs-0). In contrast, the lowest Pb concentrations were found where higher concentrations of NPs (TiO<sub>2</sub>-NPs and ZnO-NPs) were applied. Specifically, 100 mg/L TiO<sub>2</sub>-NPs significantly diminished the shoot Pb content by 84.6% and root Pb content by 45.7% as compared to control (NPs-0). TiO<sub>2</sub>-NPs at 50 mg/L treatment significantly reduced root Pb content by 30.6% and shoot Pb content by 69.5% as compared to control (NPs-0). The ZnO-NPs 100 mg/L treatment significantly decreased shoot Pb (76.7%) and root Pb (42.3%) as compared to control (NPs-0). The 50 mg/L ZnO-NPs significantly decreased Pb root content (26.3%) and Pb shoot content by 64.4% as compared

Treatment	Photosynthetic rate ( $\mu\text{ mol CO}_2\text{ m}^{-2}\text{ s}^{-1}$ )	Transpiration rate ( $\text{mol H}_2\text{O m}^{-2}\text{ s}^{-1}$ )	Water use efficiency (%)	Stomatal conductance ( $\text{mol m}^{-2}\text{ s}^{-1}$ )
NPs 0 (mg/L)	5.42 ± 0.31d	0.909 ± 0.040d	60.48 ± 5.13e	0.0106 ± 0.0011c
ZnO-NPs 25 (mg/L)	6.74 ± 0.65 cd	1.214 ± 0.78c	109.27 ± 10.5 cd	0.0255 ± 0.0012bc
TiO <sub>2</sub> -NPs 25 (mg/L)	7.46 ± 0.79bc	1.394 ± 0.149bc	114.21 ± 10.83c	0.0266 ± 0.0037b
ZnO-NPs 50 (mg/L)	8.14 ± 1.15abc	1.486 ± 0.019bc	118.43 ± 28.01bc	0.0383 ± 0.0210ab
TiO <sub>2</sub> -NPs 50 (mg/L)	9.25 ± 1.01bc	1.595 ± 0.159ab	121.28 ± 25.77b	0.0393 ± 0.0064ab
ZnO-NPs 100 (mg/L)	10.31 ± 0.94ab	1.788 ± 0.056a	125.24 ± 28.41ab	0.0404 ± 0.0010a
TiO <sub>2</sub> -NPs 100 (mg/L)	10.76 ± 2.26a	1.812 ± 0.0174a	128.0 ± 16.08a	0.0411 ± 0.0009a

**Table 1.** Effect of ZnO-NPs and TiO<sub>2</sub>-NPs on gas exchange parameters of *Brassica napus* L. grown under lead contaminated soil. Values are the means ± SD (n = 3). Different letters indicate significant differences among treatments at  $p \leq 0.05$ .

to control (NPs-0). The application at 25 mg/L TiO<sub>2</sub>-NPs and ZnO-NPs also showed a significant reduction in Pb accumulation but lower as compared to other NPs (100 mg/L) treatments.

### Effect TiO<sub>2</sub> -NPs and ZnO-NPs on nutrient profiling under Pb stress

The lowest micro and macro nutrients were recorded in the root and shoot of *Brassica napus* L. grown under only Pb stress without NPs application. While, the foliar application TiO<sub>2</sub>-NPs and ZnO-NPs significantly enhanced root and shoot zinc (Zn), iron (Fe), calcium (Ca), manganese (Mn), magnesium (Mg), and potassium (K) concentrations as compared to control (NPs-0) as depicted in (Table 2). A higher concentration of nutrient concentration was found in plants treated with the highest concentration of NPs. Specifically, 100 mg/L TiO<sub>2</sub>-NPs significantly increased root Mg (53.7%), Fe (68.4%), K (70.7%), Mn (284%), Zn (63.3%), Ca (71.6%) concentrations and shoot Mg (72.1%), Fe (79.3%) K (81.5%), Mn (62.8%), Zn (58.45%) Ca (58.2%) respectively as compared to control. Regarding ZnO-NPs, root and shoot Mg (49.5%, 93.16%), Fe (95.6%, 89.9%), K (68.6%), Mn (35.9%, 68.6%), Zn (75.7%, 78.76%) and Ca (81.5%, 69.9%), were also increased significantly in 100 mg/L ZnO-NPs treatment.

## Discussion

### Foliar application NPs improved plant growth and photosynthetic activity under Pb stress

Lead (Pb) is a non-essential and hazardous metal that hinders the normal growth and productivity of plants consequently threatening food security<sup>43</sup>. Additionally, high levels of Pb can disrupt plants metabolic systems<sup>13,44</sup>. Pb disrupts the enzyme activities that result in alterations in mineral nutrition and membrane permeability, inhibiting plant growth, photosynthesis, and morphological traits<sup>45</sup>. Several studies have highlighted the detrimental effects of Pb toxicity on crop production<sup>12,46,47</sup>. Pb toxicity reduced spinach growth<sup>48</sup> and resulted in retarded germination and low biomass in brassica plants<sup>49,50</sup>. Here in, Pb stress without NPs treatment showed poor growth in terms of shoot and root length, root dry and fresh weight, shoot dry and fresh weight, as well as number of leaves (Figs. 3, 4). The decrease in biomass might be due to the accumulation of Pb which led to excessive ROS generation and damaged plant cell membrane<sup>2</sup>. Pb toxicity inhibits photosynthetic pigment production (Fig. 5) by disrupting the Calvin cycle and carbon fixation in several agricultural plants<sup>51</sup>. Interestingly, TiO<sub>2</sub> and ZnO-NPs application had a positive impact on different aspects of plant health. In particular, the application of these NPs at a 100 mg/L application rate significantly improved plant growth characteristics, including the length of shoots and biomass (Figs. 3, 4), and in coherence with previous studies<sup>52–54</sup>. The improvement of biomass could potentially be attributed to the reduction of Pb (Fig. 8) concentration and higher mineral nutrients in NP-treated plants<sup>52</sup>.

The positive impact on growth attributes indicates an overall improvement in the physiological functions of *Brassica Napus* L. under Pb stress (Fig. 5). Increased Mg, Ca, and K content (Table.2) in NPs treated plants further supported our photosynthetic pigment results. These results are in line with many previous studies<sup>55,56</sup>. The foliar application of TiO<sub>2</sub>-NPs resulted in a substantial increase in the photosynthetic pigment in wheat and maize crops<sup>53,57</sup>. Earlier research has demonstrated that cowpea plants showed increased chlorophyll concentrations after 100 mg/L foliar application of TiO<sub>2</sub>-NPs<sup>56</sup>. TiO<sub>2</sub>-NPs influence the absorption of minerals such as Mg and Mn. Mg is necessary for the synthesis of chlorophyll, while Fe, Mn, and Zn are vital elements required for pigment production<sup>58</sup>. Due to photocatalytic properties, TiO<sub>2</sub>-NPs can improve photosynthesis efficiency<sup>59</sup>. Our results are also in agreement with a previous study by Chen et al.<sup>3</sup> who reported that 100 mg/L ZnO-NPs foliar application augmented photosynthetic activity by increasing chlorophyll concentration in plants under Cd stress. It has been observed that ZnO-NPs can boost plant Zn concentration with other essential nutrients, and regulate various physiological and biochemical activities<sup>17,52,60</sup>.

Gas exchange parameters act as stress biomarkers of metal stress in plants due to their sensitivity to environmental conditions. Higher Pb concentrations in plant leaves impede photosynthesis, hinder electron transport, and close stomata to reduce CO<sub>2</sub> assimilation<sup>61,62</sup>. The inhibitory effect of Pb on *Brassica juncea*. L by declining transpiration (*Tr*) and photosynthetic rate (*Pn*) has also been observed by Agnihotri & Seth<sup>63</sup>. In our study, it is observed that TiO<sub>2</sub>-NPs and ZnO-NPs foliar application significantly enhanced *Brassica napus* L. gas exchange parameters (Table 1). It is documented that applying TiO<sub>2</sub>-NPs increased Rubisco activity, a key enzyme in the Calvin cycle that ultimately enhances carbon dioxide fixation and boosts photosynthetic activity in plants<sup>56,64</sup>. Our findings are aligned with previous studies by Ahmad et al.<sup>65</sup> and Alhammad et al.<sup>66</sup> who reported that ZnO-NPs foliar application significantly increased photosynthetic rate, and stomatal conductance under As and Pb stress.

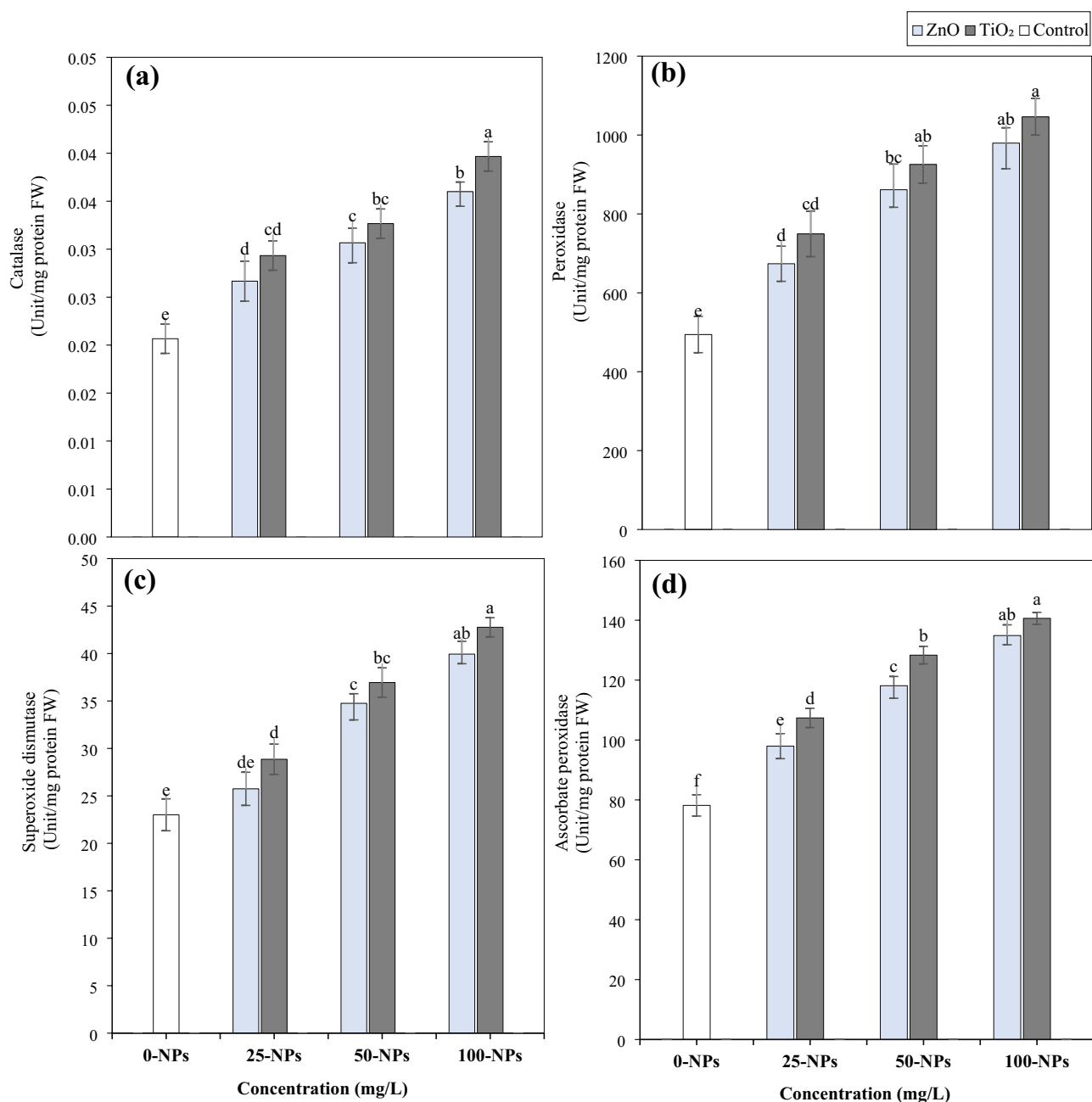


**Figure 6.** Effect of ZnO-NPs and TiO<sub>2</sub>-NPs on catalase (a), peroxidase (b), superoxide dismutase (c), and ascorbate peroxidase activities (d) in leaves of *Brassica napus* L. grown under lead contaminated soil. The vertical bar on the graph demonstrates the standard deviation. Data are presented as mean  $\pm$  SD (n = 3). Different letters on the bars indicate significant differences among treatments at  $p \leq 0.05$ .

### Foliar application of NPs improved plant antioxidant enzyme activity and reduced Pb induced oxidative damage

Numerous studies found that Pb induces oxidative stress in various plant species indicated by higher levels of MDA production<sup>44,67</sup>. MDA is generated during lipid peroxidation and triggered by ROS production<sup>68,69</sup>. Conversely, it is possible that increased levels of antioxidant activity could reduce the oxidative stress induced by HMs by scavenging excessive reactive oxygen species (ROS). High Pb concentration disrupts plant metabolism, lowering antioxidant enzyme production and causing significant harm to the plant defense system, as observed in current results<sup>70</sup>. Our results portrayed that foliar application of TiO<sub>2</sub> and ZnO-NPs reduced oxidative stress by decreasing H<sub>2</sub>O<sub>2</sub>, MDA, and EL content in plants. We observed a substantial increase in POD and CAT activities of plants which plays an important role in reducing oxidative stress and defense mechanism against Pb stress (Fig. 7). SOD scavenges O<sup>2-</sup> to H<sub>2</sub>O<sub>2</sub>, while CAT and POD decompose H<sub>2</sub>O<sub>2</sub> into water and oxygen molecules in plant cells<sup>64</sup>. Our results are confirmed by several studies that NPs can reduce the indicators of ROS (MDA,

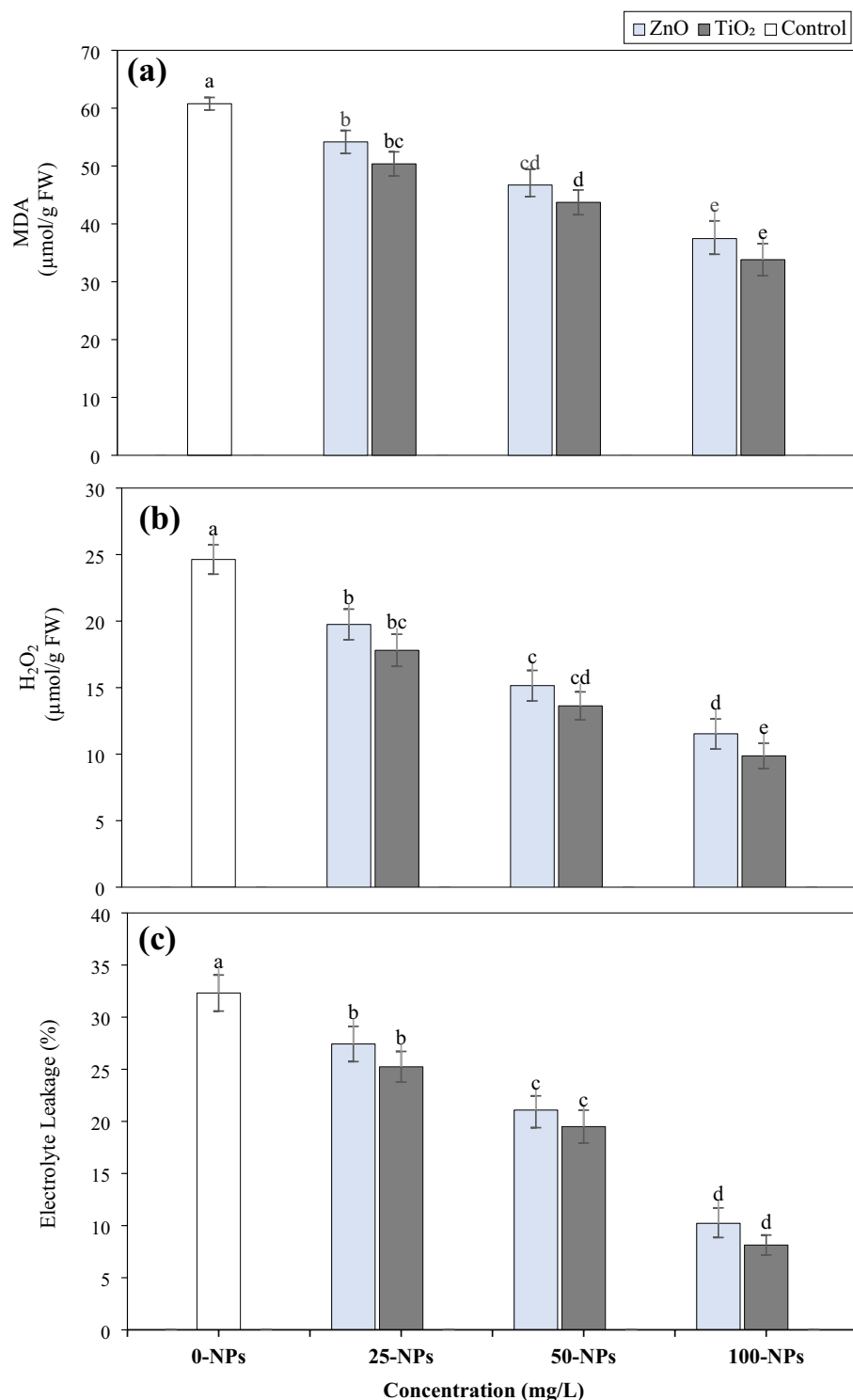


**Figure 7.** Effect of ZnO-NPs and TiO<sub>2</sub>-NPs on the accumulation of malondialdehyde (a), hydrogen peroxide (b), and electrolyte leakage (c) in leaves of *Brassica napus* L. grown under lead contaminated soil. The vertical bar on the graph demonstrates the standard deviation. Data are presented as mean ± SD (n = 3). Different letters on the bars indicate significant differences among treatments at  $p \leq 0.05$ .

H<sub>2</sub>O<sub>2</sub>, EL) in different plants and can boost resistance to oxidative stress suggesting a potential mechanism of NPs in mitigating stress induced by heavy metals<sup>8,62</sup>. Irshad et al.<sup>59</sup> and Ghouri et al.<sup>44</sup> demonstrated that TiO<sub>2</sub>-NPs reduced oxidative stress in Cd contaminated soil by increasing antioxidant enzyme activities in wheat and rice.

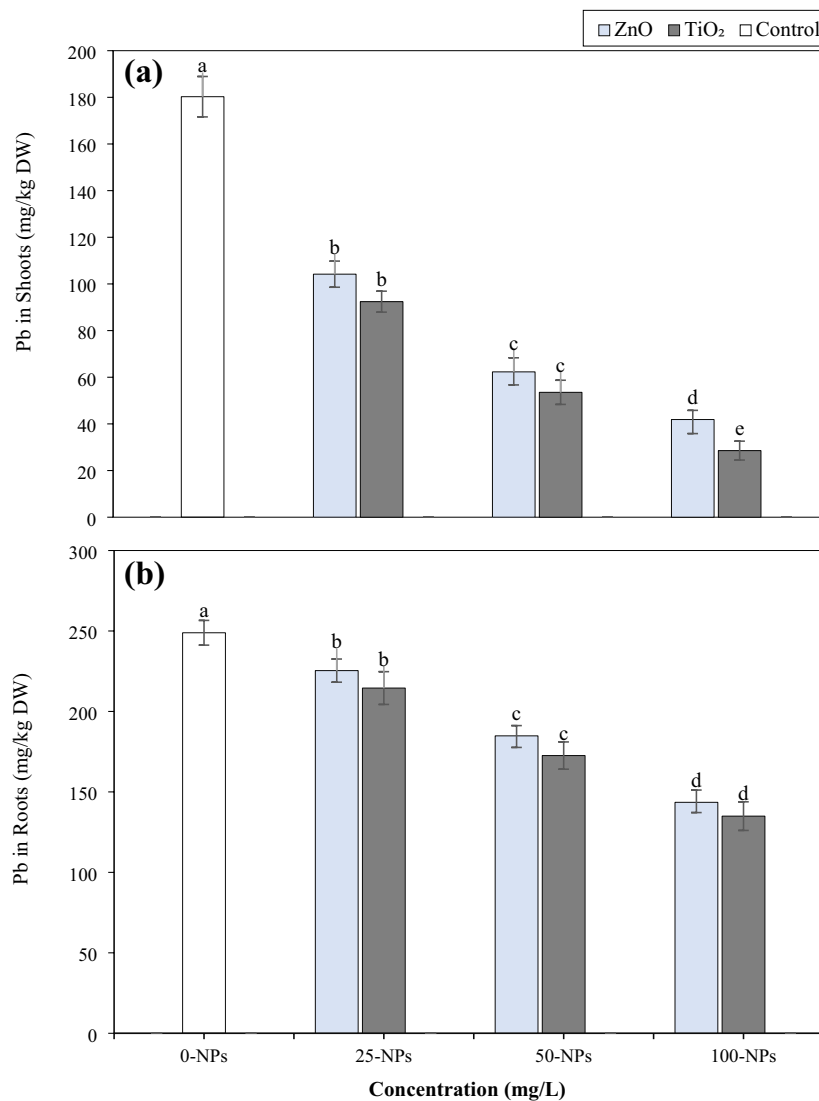


**Figure 8.** Effect of ZnO-NPs and TiO<sub>2</sub>-NPs on Lead (Pb) content in shoots (a), and Pb in roots (b) of *Brassica napus* L. grown under lead contaminated soil. The vertical bar on the graph demonstrates the standard deviation. Data are presented as mean  $\pm$  SD (n = 3). Different letters on the bars indicate significant differences among treatments at  $p \leq 0.05$ .

ZnO-NPs 50 and 100 mg/L foliar application on soybean plants for two weeks resulted in a decrease in the levels of H<sub>2</sub>O<sub>2</sub> and MDA by increasing CAT, SOD, APX, and increased soybean tolerance under metal stress<sup>65</sup>. This decrease in oxidative damage can be attributed to ZnO-NPs interaction with the plasma membrane of cells, leading to the ROS scavenging and protecting the cell membrane against oxidative damage<sup>28</sup>.

### NPs ameliorative role in Pb mitigation

Pb primarily enters the root through the root apoplast pathways or calcium ion channels. Studies have demonstrated that there is a higher accumulation of Pb in the roots compared to the shoot depending on the concentration of Pb<sup>12,62</sup>. Our results showed a higher accumulation of Pb in roots followed by shoots in plants grown under only Pb stress (Fig. 8). It is similar to the previous study in *Helianthus annuus*. L<sup>8</sup> *Oryza sativa*. L<sup>44</sup>. The observed reduction in Pb concentration in the present study might be related to the augmentation of antioxidant activities and improved biomass in the NPs treated plants, thus resulting in an overall reduction in Pb accumulation in the plants. The current findings for decreased Pb accumulation in plant roots and leaves under NPS exposure are similar to several previous studies<sup>17,50,71</sup>. TiO<sub>2</sub>-NPs exposure to rice plants decreased Pb bioaccumulation by  $\geq 80\%$  in a dose-additive manner<sup>72</sup>. The application of TiO<sub>2</sub>-NPs led to a reduction in the levels of Cd in the *Mentha piperita* L.<sup>71</sup> and wheat plants<sup>73</sup>. Kumar et al.<sup>74</sup> reported that exogenous application of TiO<sub>2</sub>-NPs created hindrance in the translocation and accumulation of metal might be ascribed to the binding of Cr transporter ions, such as sulfate or iron, with TiO<sub>2</sub>-NPs. The main mechanism by which NPs reduce HMs is by adsorption of

Treatments	Shoots					
	Macronutrients (mg g <sup>-1</sup> DW)			Micronutrients (μg g <sup>-1</sup> DW)		
	Ca	K	Mg	Mn	Fe	Zn
NPs 0 (mg/L)	15,573.53 ± 303.97f	21,319.47 ± 214.31f	13,609.80 ± 349.20 e	19.44 ± 2.97e	184.97 ± 9.31e	14.15 ± 2.07e
ZnO-NPs 25 (mg/L)	21,617.40 ± 390.62d	344,229.0 ± 285.73e	22,378.07 ± 418.20d	25.67 ± 1.29d	224.43 ± 15.77d	18.55 ± 1.07de
TiO <sub>2</sub> -NPs 25 (mg/L)	18,540.03 ± 554.95e	30,105.20 ± 446.17e	22,666.43 ± 916.29d	21.10 ± 1.71e	273.0 ± 12.62c	16.21 ± 2.52de
ZnO-NPs 50 (mg/L)	23,435.77 ± 258.88c	38,635.60 ± 310.56c	24,582.13 ± 334.06c	31.53 ± 1.32bc	309.13 ± 15.66b	36.43 ± 1.87b
TiO <sub>2</sub> -NPs 50 (mg/L)	22,341.90 ± 75.55d	36,240.37 ± 588.77d	25,217.73 ± 224.71bc	28.61 ± 0.84 cd	337.33 ± 5.84ab	20.91 ± 2.03d
ZnO-NPs 100 (mg/L)	26,296.0 ± 852.41a	42,469.60 ± 224.57a	2689.33 ± 341.26ab	35.75 ± 0.80a	361.97 ± 4.82a	64.98 ± 3.74a
TiO <sub>2</sub> -NPs 100 (mg/L)	24,650.57 ± 465.95b	40,774.40 ± 211.53b	27,121.03 ± 688.30 a	33.35 ± 1.67ab	367.57 ± 18.01a	28.03 ± 1.33c

Treatments	Roots					
	Macronutrients (mg g <sup>-1</sup> DW)			Micronutrients (μg g <sup>-1</sup> DW)		
	Ca	K	Mg	Mn	Fe	Zn
NPs 0 (mg/L)	763.73 ± 21.72f	1060.07 ± 36.77 g	9492.34 ± 319.69f	92.28 ± 2.54e	63.29 ± 10.55d	5.12 ± 1.53e
ZnO-NPs 25 (mg/L)	1243.50 ± 20.07d	1351.10 ± 27.70f	11,285.80 ± 152.09e	108.48 ± 2.28 c	114.43 ± 6.23c	7.99 ± 0.52de
TiO <sub>2</sub> -NPs 25 (mg/L)	1153.53 ± 31.57e	1470.27 ± 17.06e	11,855.43 ± 237.16e	102.59 ± 3.83d	115.92 ± 8.91c	5.60 ± 0.24e
ZnO-NPs 50 (mg/L)	1407.47 ± 12.20bc	1560.17 ± 36.52d	12,621.47 ± 215.69d	115.95 ± 1.58b	119.33 ± 6.35b	21.80 ± 0.91b
TiO <sub>2</sub> -NPs 50 (mg/L)	1357.70 ± 30.77c	1670.27 ± 43.51c	13,508.40 ± 271.60c	113.41 ± 1.01bc	121.28 ± 5.91b	9.67 ± 0.65d
ZnO-NPs 100 (mg/L)	1516.50 ± 20.62a	1797.90 ± 45.20b	14,233.70 ± 298.66b	122.73 ± 1.50 a	125.28 ± 5.91ab	32.31 ± 2.32a
TiO <sub>2</sub> -NPs 100 (mg/L)	1446.37 ± 11.95b	1894.40 ± 28.56a	15,508.03 ± 328.92a	118.81 ± 2.21ab	129.26 ± 4.46a	15.27 ± 1.51c

**Table 2.** Effect of ZnO-NPs and TiO<sub>2</sub>-NPs on nutritional profile in root and shoot of *Brassica napus* L. grown under lead contaminated soil. Values are the means ± SD (n = 3). Different letters indicate significant differences among treatments at  $p \leq 0.05$ .

metals and activation of the plant defense system<sup>75</sup>. Similarly, the efficacy of ZnO-NPs in reducing metal toxicity has been documented by previous studies<sup>23,76,77</sup>. Similar to our results previous studies showed that exogenous application of ZnO-NPs effectively reduced Cd accumulation in tomato plants Sun et al.<sup>78</sup>, wheat<sup>23</sup>, and rice<sup>79</sup> by decreasing oxidative damage. ZnO-NPs can enter through stomatal channels to the leaf epidermis and release Zn ions into the apoplast and taken up by mesophyll cells thereby reducing stress induced by HMs in plants<sup>52,75</sup>.

### Plant Nutrient Homeostasis by NPs under Pb stress

It is well known that higher Pb significantly hinders the entry of various ions to their respective absorption sites on the roots by competing with other essential nutrients and translocated through the plant system via the xylem vessels in an upward direction, together with other nutrients, and is deposited into the endodermis<sup>80</sup> (Fig. 9). In present study it is confirmed that plants under Pb stress showed lower concentration of Zn, Fe, Mg, Mn, Ca and K and higher concentration of Pb in root and shoot of *Brassica Napus* L. indicating that Pb interferes with the movement of nutrients to the above-ground part along with below ground parts as compared to the plants treated with NPs (Fig. 9). However, it has been observed that TiO<sub>2</sub>-NPs and ZnO-NPs significantly transformed the mineral balance (Table 2). A previous study showed that TiO<sub>2</sub>-NPs resulted in increased Zn levels in barley kernels<sup>81</sup>. However, some studies also reported the adverse effects of TiO<sub>2</sub>-NPs with increasing concentration<sup>82,83</sup>. TiO<sub>2</sub>-NPs surface is highly reactive, enhancing root porosity and increasing water and nutrient uptake in both normal and stressful conditions<sup>84</sup>. ZnO-NPs foliar application significantly increases the concentration of nutrients in purslane<sup>77</sup> and foxtail millet<sup>84</sup>. Similarly, in agreement with our results, a recent study by Nafees et al.<sup>18</sup> reported that ZnO-NPs foliar application significantly improved micronutrients and macronutrients in the roots and leaves of spinach under Cd stress. Zinc is a vital nutrient and can improve the plants vascular system leading to strengthened nutritional status<sup>85</sup>. The increase in plant nutrients by ZnO-NPs may also be linked to improved photosynthetic process and reduction of Pb accumulation in *Brassica Napus* L. which led to higher carbon assimilation and transpiration rate thereby improving nutrient homeostasis and overall plant development.

### Conclusion

The present study has highlighted the potential impact of TiO<sub>2</sub>-NPs and ZnO-NPs on *Brassica napus* L. under Pb stress. The foliar application of 100 TiO<sub>2</sub>-NPs and ZnO-NPs significantly enhanced *Brassica napus* L. growth and physiology. TiO<sub>2</sub>-NPs and ZnO-NPs reduced oxidative stress by upregulation of leaf antioxidant enzyme activity. Furthermore, these NPs significantly reduced Pb uptake in dose dose-dependent manner by improving plant defensive mechanism. Our study demonstrated that the application of NPs (TiO<sub>2</sub>-NPs and ZnO-NPs) enhanced Zn, Fe, Mg, Mn, Ca, and K in *Brassica napus* L. root and shoot by reducing Pb concentration in plant parts and maintaining ionic balance. Overall study concluded that both TiO<sub>2</sub>-NPs and ZnO-NPs proved to be efficient in mitigating Pb induced toxicity and nutrient strengthening under metal stress. Further studies are needed to focus on gene expression related to Pb uptake in plants by TiO<sub>2</sub>-NPs and ZnO-NPs under different conditions in fields.

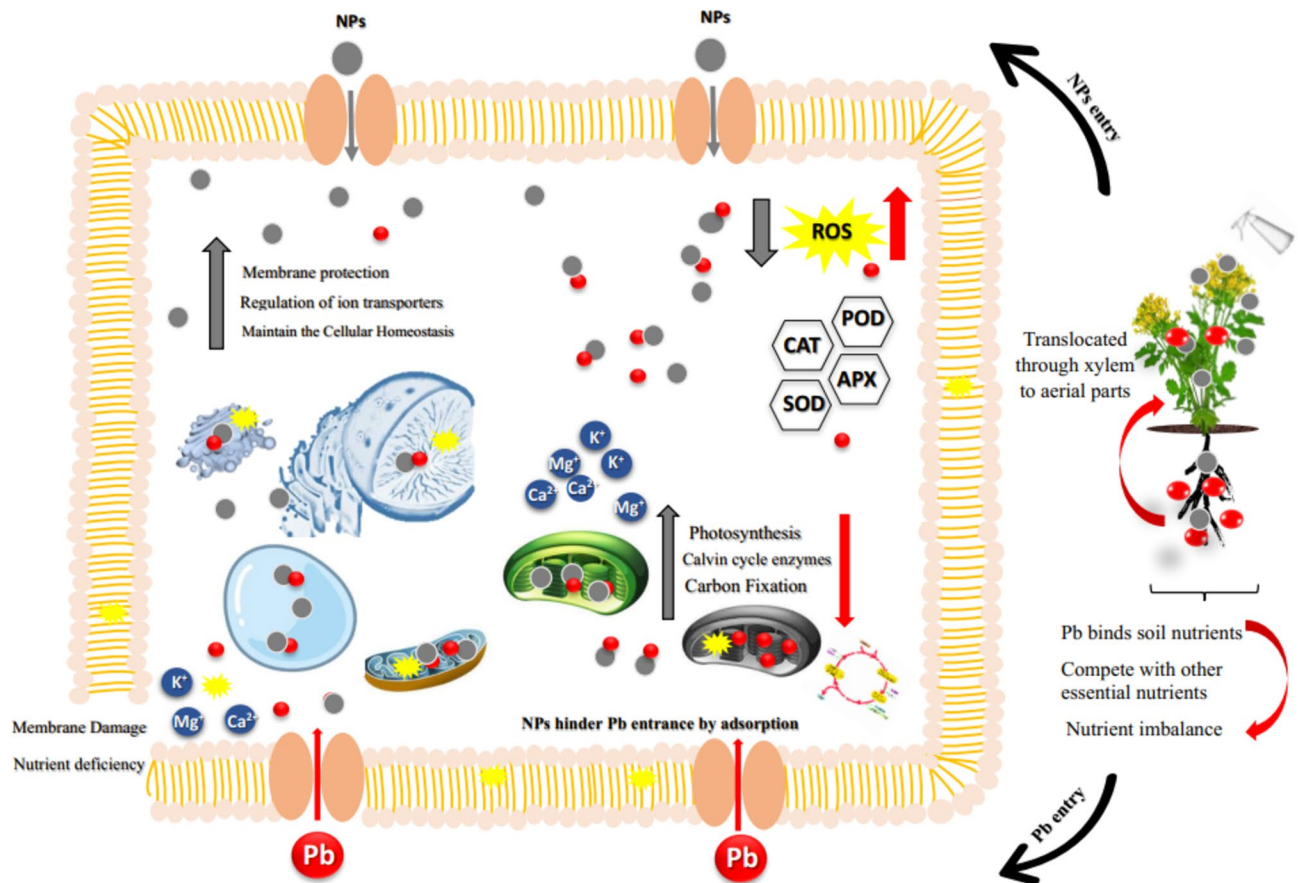


**Figure 9.** Model representing the mechanistic role of NPs to alleviate Pb toxicity and nutrient strengthening.

### Data availability

All data generated or analyzed during the study are included in this article.

Received: 11 March 2024; Accepted: 13 August 2024

Published online: 21 August 2024

### References

- Rizwan, M. *et al.* Cadmium stress in rice: toxic effects, tolerance mechanisms, and management: A critical review. *Environ. Sci. Pollut. Res.* **23**, 17859–17879. <https://doi.org/10.1007/s11356-016-6436-4> (2016).
- Aborisade, M. A. *et al.* Remediation of soil polluted with Pb and Cd and alleviation of oxidative stress in *Brassica rapa* plant using nanoscale zerovalent iron supported with coconut-husk biochar. *J. Plant Physiol.* <https://doi.org/10.1016/j.jplph.2023.154023> (2023).
- Chen, F. *et al.* Effect of titanium dioxide nanoparticles and co-composted biochar on growth and Cd uptake by wheat plants: A field study. *Environ. Res.* **231**, 116057. <https://doi.org/10.1016/j.envres.2023.116057> (2023).
- Chen, F. *et al.* Combined effects of zinc oxide nanoparticles and melatonin on wheat growth, chlorophyll contents, cadmium (Cd) and zinc uptake under Cd stress. *Sci. Total Environ.* **864**, 161061. <https://doi.org/10.1016/j.scitotenv.2022.161061> (2023).
- Rashid, A. *et al.* Heavy metal contamination in agricultural soil: Environmental pollutants affecting crop health. *Agronomy* **13**(6), 1521. <https://doi.org/10.3390/agronomy13061521> (2023).
- Ahmad, S. *et al.* Combined application of biochar and metal-tolerant bacteria alleviates cadmium toxicity by modulating the antioxidant defense mechanism and physicochemical attributes in rice (*Oryza sativa* L.) grown in cadmium-contaminated soil. *Plant Stress* **11**, 100348. <https://doi.org/10.1016/j.stress.2024.100348> (2024).
- Nag, R. & Cummins, E. Human health risk assessment of lead (Pb) through the environmental-food pathway. *Sci. Total Environ.* **810**, 151168. <https://doi.org/10.1016/j.scitotenv.2021.151168> (2022).
- Mahamood, M. N. *et al.* An assessment of the efficacy of biochar and zero-valent iron nanoparticles in reducing lead toxicity in wheat (*Triticum aestivum* L.). *Environ. Pollut.* **319**, 120979. <https://doi.org/10.1016/j.envpol.2022.120979> (2023).
- Nas, F. S. & Ali, M. The effect of lead on plants in terms of growing and biochemical parameters: a review. *MOJ Ecol. Environ. Sci.* **3**(4), 265–268. <https://doi.org/10.15406/mojes.2018.03.00098> (2018).
- Mitra, A., Chatterjee, S., Voronina, A. V., Walther, C. & Gupta, D. K. Lead toxicity in plants: A review. *Lead Plants Environ.* <https://doi.org/10.1007/978-3-030-21638-26> (2020).
- Debnath, B., Singh, W. S. & Manna, K. Sources and toxicological effects of lead on human health India. *J. Med. Spec.* **10**(2), 66–71. <https://doi.org/10.4103/INJMS.INJMS3018> (2019).
- Fatemi, H., Pour, B. E. & Rizwan, M. Isolation and characterization of lead (Pb) resistant microbes and their combined use with silicon nanoparticles improved the growth, photosynthesis and antioxidant capacity of coriander (*Coriandrum sativum* L.) under Pb stress. *Environ. Pollut.* **266**, 114982. <https://doi.org/10.1016/j.envpol.2020.114982> (2020).
- Zulfikar, U. *et al.* Lead toxicity in plants: Impacts and remediation. *J. Environ. Manag.* **250**, 10955. [https://doi.org/10.1007/978-3-031-46146-0\\_9](https://doi.org/10.1007/978-3-031-46146-0_9) (2019).



14. Khanam, R. *et al.* Metal (loid)s (As, Hg, Se, Pb and Cd) in paddy soil: Bioavailability and potential risk to human health. *Sci. Total Environ.* **699**, 134330. <https://doi.org/10.1016/j.scitotenv.2019.134330> (2020).
15. Ali, S. *et al.* Combined use of biochar and zinc oxide nanoparticlefoliar spray improved the plant growth and decreased the cadmium accumulation in rice (*Oryza sativa* L.) plant. *Environ. Sci. Pollut. Res.* **26**, 11288–11299. <https://doi.org/10.1007/s11356-019-04554-y> (2019).
16. Kumar, D. *et al.* Review on interactions between nanomaterials and phytohormones: Novel perspectives and opportunities for mitigating environmental challenges. *Plant Sci.* **340**, 111964. <https://doi.org/10.1016/j.plantsci.2023.111964> (2024).
17. Ahmad, S. *et al.* Chromium-resistant *Staphylococcus aureus* alleviates chromium toxicity by developing synergistic relationships with zinc oxide nanoparticles in wheat. *Ecotoxicol. Environ. Saf.* **230**, 113142. <https://doi.org/10.1016/j.ecoenv.2021.113142> (2022).
18. Nafees, M. *et al.* Mechanism and synergistic effect of sulfadiazine (SDZ) and cadmium toxicity in spinach (*Spinacia oleracea* L.) and its alleviation through zinc fortification. *J. Hazard. Mater.* **464**, 132903. <https://doi.org/10.1016/j.jhazmat.2023.132903> (2024).
19. Yan, A. & Chen, Z. Impacts of silver nanoparticles on plants: a focus on the phytotoxicity and underlying mechanism. *Int. J. Mol. Sci.* **20**(5), 1003. <https://doi.org/10.3390/ijms20051003> (2019).
20. Silva, S., Dias, M. C. & Silva, A. M. Titanium and zinc based nanomaterials in agriculture: A promising approach to deal with (a) biotic stresses?. *Toxics* **10**(4), 172. <https://doi.org/10.3390/toxics10040172> (2022).
21. Daghan, H., Gülmezoglu, N., Köleli, N. & Karakaya, B. Impact of titanium dioxide nanoparticles (TiO<sub>2</sub>-NPs) on growth and mineral nutrient uptake of wheat (*Triticum vulgare* L.). *Biotech. Stud.* **29**(2), 69–76. <https://doi.org/10.38042/biost.2020.29.02.03> (2020).
22. Gupta, N. *et al.* Seed priming with ZnO and Fe<sub>3</sub>O<sub>4</sub> nanoparticles alleviate the lead toxicity in *Basella alba* L. through reduced lead uptake and regulation of ROS. *Plants* **11**, 2227. <https://doi.org/10.3390/plants11172227> (2022).
23. Ghouri, F. *et al.* The protective role of tetraploidy and nanoparticles in arsenic-stressed rice: Evidence from RNA sequencing, ultrastructural and physiological studies. *J. Hazard. Mater.* **458**, 132019. <https://doi.org/10.1016/j.jhazmat.2023.132019> (2023).
24. Bakshi, M. & Kumar, A. Co-application of TiO<sub>2</sub> nanoparticles and hyperaccumulator *Brassica juncea* L. for effective Cd removal from soil: Assessing the feasibility of using nano-phytoremediation. *J. Environ. Manage.* **341**, 118005. <https://doi.org/10.1016/j.jenvman.2023.118005> (2023).
25. Kumar, D. *et al.* Comparative investigation on chemical and green synthesized titanium dioxide nanoparticles against chromium (VI) stress eliciting differential physiological, biochemical, and cellular attributes in *Helianthus annuus* L. *Sci. Total Environ.* **930**, 172413. <https://doi.org/10.1016/j.scitotenv.2024.172413> (2024).
26. Arshad, M. *et al.* Multi-element uptake and growth responses of Rice (*Oryza sativa* L.) to TiO<sub>2</sub> nanoparticles applied in different textured soils. *Ecotoxicol. Environ. Saf.* **215**, 112149. <https://doi.org/10.1016/j.ecoenv.2021.112149> (2021).
27. Hassan, M. *et al.* The role of zinc to mitigate heavy metals toxicity in crops. *Front. Environ. Sci.* **10**, 990223. <https://doi.org/10.3389/fenvs.2022.990223> (2022).
28. Jalil, S. *et al.* Zinc oxide nanoparticles mitigated the arsenic induced oxidative stress through modulation of physio-biochemical aspects and nutritional ions homeostasis in rice (*Oryza sativa* L.). *Chemosphere.* **338**, 139566. <https://doi.org/10.1016/j.chemosphere.2023.139566> (2023).
29. Faizan, M., Bhat, J. A., Hessini, K., Yu, F. & Ahmad, P. Zinc oxide nanoparticles alleviates the adverse effects of cadmium stress on *Oryza sativa* via modulation of the photosynthesis and antioxidant defense system. *Ecotoxicol. Environ. Saf.* **220**, 112401. <https://doi.org/10.1016/j.ecoenv.2021.112401> (2021).
30. Feigl, G. *et al.* Different zinc sensitivity of Brassica organs is accompanied by distinct responses in protein nitration level and pattern. *Ecotoxicol. Environ. Saf.* **125**, 141–152. <https://doi.org/10.1016/j.ecoenv.2015.12.006> (2016).
31. Poursani, A. S. *et al.* The synthesis of nano TiO<sub>2</sub> and its use for removal of lead ions from aqueous solution. *J. Water Resource Prot.* **8**(04), 438. <https://doi.org/10.4236/jwarp.2016.84037> (2016).
32. Vishwakarma, A. & Singh, S. P. Synthesis of zinc oxide nanoparticle by sol-gel method and study its characterization. *Int. J. Res. Appl. Sci. Eng. Technol.* **8**(4), 1625–1627. <https://doi.org/10.22214/ijraset.2020.4265> (2020).
33. Lichtenthaler, H. K. Chlorophylls and carotenoids: Pigments of photosynthetic biomembranes. *Method Enzymol.* **148**, 350–382. [https://doi.org/10.1016/0076-6879\(87\)48036-1](https://doi.org/10.1016/0076-6879(87)48036-1) (1987).
34. Zhang, X.Z. The measurement and mechanism of lipid peroxidation and SOD, POD and CAT activities in biological system. *Res. Method. Crop Physiol.* 208–211 (1992).
35. Aebi, H. Catalase in vitro. *Method. Enzymol.* **105**, 121–126. [https://doi.org/10.1016/S0076-6879\(84\)05016-3](https://doi.org/10.1016/S0076-6879(84)05016-3) (1984).
36. Nakano, Y. & Asada, K. Hydrogen peroxide is scavenged by ascorbate-specific peroxidase in spinach chloroplasts. *Plant Cell Physiol.* **22**(5), 867–880. <https://doi.org/10.1093/oxfordjournals.pcp.a076232> (1981).
37. Heath, R. L. & Packer, L. Photoperoxidation in isolated chloroplasts: I. Kinetics and stoichiometry of fatty acid peroxidation. *Arch. Biochem. Biophys.* **125**(1), 189–198. [https://doi.org/10.1016/0003-9861\(68\)90654-1](https://doi.org/10.1016/0003-9861(68)90654-1) (1968).
38. Jana, S. & Choudhuri, M. A. Senescence in submerged aquatic angiosperms: Effects of heavy metals. *N. Phytol.* **90**(3), 477–484. <https://doi.org/10.1111/j.1469-8137.1982.tb04480.x> (1982).
39. Dionisio-Sese, M. L. & Tobita, S. Antioxidant responses of rice seedlings to salinity stress. *Plant Sci.* **135**(1), 1–9. [https://doi.org/10.1016/S0168-9452\(98\)00025-9](https://doi.org/10.1016/S0168-9452(98)00025-9) (1998).
40. Rehman, M. Z. U. *et al.* Effect of inorganic amendments for in situ stabilization of cadmium in contaminated soils and its phyto-availability to wheat and rice under rotation. *Environ. Sci. Pollut. Res.* **22**, 16897–16906. <https://doi.org/10.1007/s11356-015-4883-y> (2015).
41. Xiao, X. *et al.* The high efficient catalytic properties for thermal decomposition of ammonium perchlorate using mesoporous ZnCo<sub>2</sub>O<sub>4</sub> rods synthesized by oxalate co-precipitation method. *Sci. Rep.* **8**(1), 7571. <https://doi.org/10.1038/s41598-018-26022-2> (2018).
42. Viana, M. M., Soares, V. F. & Mohallem, N. D. S. Synthesis and characterization of TiO<sub>2</sub> nanoparticles. *Ceram. Int.* **36**(7), 2047–2053. <https://doi.org/10.1016/j.ceramint.2010.04.006> (2010).
43. Pujari, M., & Kapoor, D. Heavy metals in the ecosystem: sources and their effects. In: Heavy Metals in the Environment: Impact, Assessment, and Remediation, Elsevier <https://doi.org/10.1016/B978-0-12-821656-9.00001-8>. (2020)
44. Ghouri, F. *et al.* Alleviated lead toxicity in rice plant by co-augmented action of genome doubling and TiO<sub>2</sub> nanoparticles on gene expression, cytological and physiological changes. *Sci. Total Environ.* **911**, 168709. <https://doi.org/10.1016/j.scitotenv.2023.168709> (2024).
45. Guo, G., Lei, M., Wang, Y., Song, B. & Yang, J. Accumulation of As, Cd, and Pb in sixteen wheat cultivars grown in contaminated soils and associated health risk assessment. *Int. J. Environ. Res. Public Health* **15**, 2601. <https://doi.org/10.3390/ijerph15112601> (2018).
46. Islam, E. *et al.* Effect of Pb toxicity on leaf growth, physiology and ultrastructure in the two ecotypes of *Elsholtzia argyi*. *J. Hazard. Mater.* **154**(1–3), 914–926. <https://doi.org/10.1016/j.jhazmat.2007.10.121> (2008).
47. Shakoor, M. B. *et al.* Citric acid improves lead (Pb) phytoextraction in *Brassica napus* L. by mitigating Pb-induced morphological and biochemical damages. *Ecotoxicol. Environ. Saf.* **109**, 38–47. <https://doi.org/10.1016/j.ecoenv.2014.07.033> (2014).
48. Zafar-ul-Hye, M. *et al.* Potential role of compost mixed biochar with rhizobacteria in mitigating lead toxicity in spinach. *Sci. Rep.* **10**(1), 12159. <https://doi.org/10.1038/s41598-020-69183-9> (2020).
49. Kanwal, A. *et al.* Effect of industrial wastewater on wheat germination, growth, yield, nutrients and bioaccumulation of lead. *Sci. Rep.* **10**(1), 11361. <https://doi.org/10.1038/s41598-020-69183-9> (2020).

50. Bassegio, C. *et al.* Growth and accumulation of Pb by roots and shoots of *Brassica juncea* L. *Int. J. Phytoremediation*. **22**(2), 134–139. <https://doi.org/10.1080/15226514.2019.1647406> (2020).
51. Khan, A., Khan, S., Khan, M. A., Qamar, Z. & Waqas, M. The uptake and bioaccumulation of heavy metals by food plants, their effects on plants nutrients, and associated health risk: A review. *Environ. Sci. Pollut. Res.* **22**, 13772–13799. <https://doi.org/10.1007/s11356-015-4881-0> (2015).
52. Rizwan, M. *et al.* Zinc and iron oxide nanoparticles improved the plant growth and reduced the oxidative stress and cadmium concentration in wheat. *Chemosphere* **214**, 269–277. <https://doi.org/10.1016/j.chemosphere.2018.09.120> (2019).
53. Lian, J. *et al.* Foliar spray of combined metal-oxide nanoparticles alters the accumulation, translocation and health risk of Cd in wheat (*Triticum aestivum* L.). *J. Hazard. Mater.* **440**, 129857. <https://doi.org/10.1016/j.jhazmat.2022.129857> (2022).
54. Ogunkunle, C. O. *et al.* Cadmium toxicity in cowpea plant: Effect of foliar intervention of nano-TiO<sub>2</sub> on tissue Cd bioaccumulation, stress enzymes and potential dietary health risk. *J. Biotechnol.* **310**, 54–61. <https://doi.org/10.1016/j.jbiotec.2020.01.009> (2020).
55. Ahmed, K. B. *et al.* Comparative effect of foliar application of silicon, titanium and zinc nanoparticles on the performance of vetiver-a medicinal and aromatic plant. *Silicon* **15**(1), 153–166. <https://doi.org/10.1007/s12633-022-02007-9> (2023).
56. Gao, J. *et al.* Effects of nano-TiO<sub>2</sub> on photosynthetic characteristics of *Ulmus elongata* seedlings. *Environ. Pollut.* **176**, 63–70. <https://doi.org/10.1016/j.envpol.2013.01.027> (2013).
57. Irshad, M. A. *et al.* Effect of green and chemically synthesized titanium dioxide nanoparticles on cadmium accumulation in wheat grains and potential dietary health risk: A field investigation. *J. Hazard. Mater.* **415**, 125585. <https://doi.org/10.1016/j.jhazmat.2021.125585> (2021).
58. Kumar, D. *et al.* Comparative investigation on chemical and green synthesized titanium dioxide nanoparticles against chromium (VI) stress eliciting differential physiological, biochemical, and cellular attributes in *Helianthus annuus* L. *Sci. Total Environ.* **930**, 172413. <https://doi.org/10.1016/j.jhazmat.2021.125585> (2024).
59. Vatankhah, A. *et al.* Plants exposed to titanium dioxide nanoparticles acquired contrasting photosynthetic and morphological strategies depending on the growing light intensity: A case study in radish. *Sci. Rep.* **13**(1), 5873. <https://doi.org/10.1038/s41598-023-32466-y> (2023).
60. Raghieb, F., Naikoo, M. I., Khan, F. A., Alyemeni, M. N. & Ahmad, P. Interaction of ZnO nanoparticle and AM fungi mitigates Pb toxicity in wheat by upregulating antioxidants and restricted uptake of Pb. *J. Biotechnol.* **323**, 254–263. <https://doi.org/10.1016/j.jbiotec.2020.09.003> (2020).
61. Sharma, A. *et al.* Photosynthetic response of plants under different abiotic stresses: A review. *J. Plant Growth Regul.* **39**, 509–531. <https://doi.org/10.1007/s00344-019-10018-x> (2020).
62. Sha, S. *et al.* Toxic effects of Pb on *Spirodela polyrrhiza* (L.): Subcellular distribution, chemical forms, morphological and physiological disorders. *Ecotoxicol. Environ. Saf.* **181**, 146–154. <https://doi.org/10.1016/j.ecoenv.2019.05.085> (2019).
63. Agnihotri, A. & Seth, C. S. Does jasmonic acid regulate photosynthesis, clastogenicity, and phytochelatin in *Brassica juncea* L. in response to Pb-subcellular distribution. *Chemosphere* **243**, 125361. <https://doi.org/10.1016/j.chemosphere.2019.125361> (2020).
64. Ali, S., Mehmood, A. & Khan, N. Uptake, translocation, and consequences of nanomaterials on plant growth and stress adaptation. *J. Nanomater.* <https://doi.org/10.1155/2021/6677616> (2021).
65. Ahmad, P. *et al.* Zinc oxide nanoparticles application alleviates arsenic (As) toxicity in soybean plants by restricting the uptake of as and modulating key biochemical attributes, antioxidant enzymes, ascorbate-glutathione cycle and glyoxalase system. *Plants* **9**(7), 825. <https://doi.org/10.3390/plants9070825> (2020).
66. Alhammad, B. A., Ahmad, A. & Seleiman, M. F. Nano-hydroxyapatite and ZnO-NPs Mitigate Pb Stress in maize. *Agronomy* **13**(4), 1174. <https://doi.org/10.3390/agronomy13041174> (2023).
67. Ashraf, U. Alterations in growth, oxidative damage, and metal uptake of five aromatic rice cultivars under lead toxicity. *Plant Physiol. Biochem.* **115**, 461–471. <https://doi.org/10.1016/j.plaphy.2017.04.019> (2017).
68. Omidifar, N. *et al.* The modulatory potential of herbal antioxidants against oxidative stress and heavy metal pollution: Plants against environmental oxidative stress. *Environ. Sci. Pollut. Res.* <https://doi.org/10.1007/s11356-021-16530-6> (2021).
69. Tripathi, D. K. *et al.* Nitric oxide ameliorates zinc oxide nanoparticles phytotoxicity in wheat seedlings: implication of the ascorbate–glutathione cycle. *Front. Plant Sci.* **8**, 1. <https://doi.org/10.3389/fpls.2017.00001> (2017).
70. Collin, S. *et al.* Bioaccumulation of lead (Pb) and its effects in plants: A review. *J. Hazard. Mater. Lett.* <https://doi.org/10.1016/j.hazl.2022.100064> (2022).
71. Mohammadi, H. *et al.* Unraveling the influence of TiO<sub>2</sub> nanoparticles on growth, physiological and phytochemical characteristics of *Mentha piperita* L. in cadmium-contaminated soil. *Sci. Rep.* **13**(1), 22280. <https://doi.org/10.1038/s41598-023-49666-1> (2023).
72. Cai, F. *et al.* Impact of TiO<sub>2</sub> nanoparticles on lead uptake and bioaccumulation in rice (*Oryza sativa* L.). *NanoImpact* **5**, 101–108. <https://doi.org/10.1016/j.impact.2017.01.006> (2017).
73. Chen, F. *et al.* Effect of titanium dioxide nanoparticles and co-composted biochar on growth and Cd uptake by wheat plants: A field study. *Environ. Pollut.* **231**, 116057. <https://doi.org/10.1016/j.envres.2023.116057> (2023).
74. Kumar, D., Dhankher, O. P., Tripathi, R. D. & Seth, C. S. Titanium dioxide nanoparticles potentially regulate the mechanism (s) for photosynthetic attributes, genotoxicity, antioxidants defense machinery, and phytochelatin synthesis in relation to hexavalent chromium toxicity in *Helianthus annuus* L. *J. Hazard. Mater.* **454**, 131418. <https://doi.org/10.1016/j.jhazmat.2023.131418> (2023).
75. Zhou, P. *et al.* Application of nanoparticles alleviates heavy metals stress and promotes plant growth: An overview. *Nanomaterial* **11**(1), 26. <https://doi.org/10.3390/nano11010026> (2020).
76. Sharifan, H., Moore, J. & Ma, X. Zinc oxide (ZnO) nanoparticles elevated iron and copper contents and mitigated the bioavailability of lead and cadmium in different leafy greens. *Ecotoxicol. Environ. Saf.* **191**, 110177. <https://doi.org/10.1016/j.ecoenv.2020.110177> (2020).
77. Pishkar, L., Yousefi, S. & Iranbakhsh, A. Foliar application of Zinc oxide nanoparticles alleviates cadmium toxicity in purslane by maintaining nutrients homeostasis and improving the activity of antioxidant enzymes and glyoxalase system. *Ecotoxicology* **31**(4), 667–678. <https://doi.org/10.1007/s10646-022-02533-7> (2022).
78. Sun, L. *et al.* Mitigation mechanism of zinc oxide nanoparticles on cadmium toxicity in tomato. *Front. Plant Sci.* **14**, 1162372. <https://doi.org/10.3389/fpls.2023.1162372> (2023).
79. Bashir, A. *et al.* Effect of composted organic amendments and zinc oxide nanoparticles on growth and cadmium accumulation by wheat; a life cycle study. *Environ. Sci. Pollut. Res.* **27**, 23926–23936. <https://doi.org/10.1007/s11356-020-08739-8> (2020).
80. Dubey, R., Gupta, D. K. & Sharma, G. K. Chemical stress on plants. *New Front. Stress Manag. Durable Agric.* [https://doi.org/10.1007/978-981-15-1322-0\\_7](https://doi.org/10.1007/978-981-15-1322-0_7) (2020).
81. Pošćić, F. *et al.* Effects of cerium and titanium oxide nanoparticles in soil on the nutrient composition of barley (*Hordeum vulgare* L.) kernels. *Int. J. Environ. Res. Public Health.* **13**(6), 577. <https://doi.org/10.3390/ijerph13060577> (2016).
82. Hu, J. *et al.* TiO<sub>2</sub> nanoparticle exposure on lettuce (*Lactuca sativa* L.): Dose-dependent deterioration of nutritional quality. *Environ. Sci. Nano* **7**(2), 501–513. <https://doi.org/10.1039/C9EN01215J> (2020).
83. Alharby, H. F. *et al.* Effect of gibberellic acid and titanium dioxide nanoparticles on growth, antioxidant defense system and mineral nutrient uptake in wheat. *Ecotoxicol. Environ. Saf.* **221**, 112436. <https://doi.org/10.1016/j.ecoenv.2021.112436> (2021).
84. Raliya, R. *et al.* Mechanistic evaluation of translocation and physiological impact of titanium dioxide and zinc oxide nanoparticles on the tomato (*Solanum lycopersicum* L.) plant. *Metallomics* **7**(12), 1584–1594. <https://doi.org/10.1039/c5mt00168d> (2015).

85. Kolenčik, M. G. *et al.* Effect of foliar spray application of zinc oxide nanoparticles on quantitative, nutritional, and physiological parameters of foxtail millet (*Setaria italica* L.) under field conditions. *Nanomater.* **9**(11), 1559. <https://doi.org/10.3390/nano9111559> (2019).
86. Lv, J. *et al.* Accumulation, speciation and uptake pathway of ZnO nanoparticles in maize. *Environ. Sci. Nano* **2**(1), 68–77. <https://doi.org/10.1039/C4EN00064A> (2015).

### Acknowledgements

The authors wish to acknowledge the State Key Laboratory of Pollution Control and Resource Reuse, School of the Environment, Nanjing University and Environmental Toxicology & Chemistry laboratory, Government College University, Faisalabad. The authors express their sincere appreciation to the Researchers Supporting Project Number (RSP2024R48), King Saud University, Riyadh, Saudi Arabia.

### Author contributions

A.K.S.: Performed the design of experiment, Formal analysis, carried out the experiment and original drafted the manuscript. S.A.: Formal analysis and writing—review and editing. S.O.A.: Formal analysis. A.A.: Revising it critically for intellectual content. K.A.A.G.: Funding Acquisition, writing—review and editing. M.A.A.: investigation. A.T.: writing—review. S.A. and P.K.S.: Supervision, Experiment design, Resources, Investigation.

### Competing interests

The authors declare no competing interests.

### Additional information

**Correspondence** and requests for materials should be addressed to S.A. or P.K.S.

**Reprints and permissions information** is available at [www.nature.com/reprints](http://www.nature.com/reprints).

**Publisher's note** Springer Nature remains neutral with regard to jurisdictional claims in published maps and institutional affiliations.

**Open Access** This article is licensed under a Creative Commons Attribution 4.0 International License, which permits use, sharing, adaptation, distribution and reproduction in any medium or format, as long as you give appropriate credit to the original author(s) and the source, provide a link to the Creative Commons licence, and indicate if changes were made. The images or other third party material in this article are included in the article's Creative Commons licence, unless indicated otherwise in a credit line to the material. If material is not included in the article's Creative Commons licence and your intended use is not permitted by statutory regulation or exceeds the permitted use, you will need to obtain permission directly from the copyright holder. To view a copy of this licence, visit <http://creativecommons.org/licenses/by/4.0/>.

© The Author(s) 2024